

Zeroth-Order Regularized Optimization (ZORO): Approximately Sparse Gradients and Adaptive Sampling

HanQin Cai¹, Daniel Mckenzie¹, Wotao Yin^{2,1}, and Zhenliang Zhang²

¹Department of Mathematics,
University of California, Los Angeles,
Los Angeles, CA, USA.

²Damo Academy,
Alibaba US,
Seattle, WA, USA.

August 7, 2022

Abstract

We consider the problem of minimizing a high-dimensional objective function, which may include a regularization term, using only (possibly noisy) evaluations of the function. Such optimization is also called derivative-free, zeroth-order, or black-box optimization. We propose a new **Zeroth-Order Regularized Optimization** method, dubbed ZORO. When the underlying gradient is approximately sparse at an iterate, ZORO needs very few objective function evaluations to obtain a new iterate that decreases the objective function. We achieve this with an adaptive, randomized gradient estimator, followed by an inexact proximal-gradient scheme. Under a novel approximately sparse gradient assumption and various different convex settings, we show the (theoretical and empirical) convergence rate of ZORO is only logarithmically dependent on the problem dimension. Numerical experiments show that ZORO outperforms the existing methods with similar assumptions, on both synthetic and real datasets.

1 Introduction

Zeroth-order optimization, also known as derivative-free or black-box optimization, appears in a wide range of applications where either the objective function is implicit or the objective gradient is impossible or too expensive to compute. These applications include structured prediction (Taskar et al., 2005), reinforcement learning (Choromanski et al., 2018), bandit optimization (Flaxman et al., 2004; Shamir, 2013) optimal setting search in material science experiments (Nakamura et al., 2017), adversarial attacks on neural networks (Kurakin et al., 2016; Papernot et al., 2017), and hyper-parameter tuning (Snoek et al., 2012).

Email addresses: hqcai@math.ucla.edu (H.Q. Cai), mckenzie@math.ucla.edu (D. Mckenzie), wotao.yin@alibaba-inc.com (W. Yin), and zhenliang.zhang@alibaba-inc.com (Z. Zhang).

Formally, the goal of zeroth-order optimization is to solve the minimization problem:

$$\underset{x \in \mathcal{X} \subseteq \mathbb{R}^d}{\text{minimize}} f(x) \quad (1)$$

with access to (potentially noisy) function evaluations only. These function evaluations are acquired through an *oracle*:

$$E_f(x) = f(x) + \xi, \quad (2)$$

where ξ is the unknown oracle noise. When we call the oracle with an input x , it returns $E_f(x)$ in which ξ may or may not change every time. Zeroth-order methods are typically evaluated in terms of the number of required oracle queries.

One popular approach to zeroth-order optimization is to use oracle queries to estimate the gradient and then apply a first-order optimization method (Kiefer et al., 1952; Spall, 1998; Nesterov & Spokoiny, 2011). Generally speaking, gradient estimation based methods work well with convex objective functions (Agarwal et al., 2010; Duchi et al., 2015; Wang et al., 2018), and also suitable with some non-convex models (Nesterov & Spokoiny, 2011; Ghadimi & Lan, 2013) and parallel optimization (Lian et al., 2016; Gu et al., 2018).

Nevertheless, these methods suffer from a mild curse of dimensionality. Compared with the analogous first-order methods, zeroth-order methods employing gradient estimators typically have a linear factor of the problem dimension, d , in their oracle complexity (Jamieson et al., 2012; Duchi et al., 2015). This is problematic when d is very large.

To reduce query complexity in the high dimensional case, (Wang et al., 2018) and (Balasubramanian & Ghadimi, 2018) introduced methods that exploit *exact sparsity* of the gradients. That is, $\nabla f(x)$ has only a few non-zero entries at any point x . Their methods enjoy a query complexity that is polynomially dependent on $\log(d)$ —a significant saving in the high dimensional case. However, their exact sparsity assumption often fails to hold in practice. In fact, (Balasubramanian & Ghadimi, 2018) has no empirical results, and (Wang et al., 2018) provides only experiments on synthetic datasets. Hence, we argue that *approximate sparsity*, in particular compressibility (see Assumption 1.b) is a more practical assumption. For example, in hyper-parameter tuning, the performance is often sensitive to only a few hyper-parameters, so they tend to carry more significant weights in gradients. But, less-sensitive ones also have non-zero weights and need to be tuned. To clarify, approximately -sparse gradients are can be completely dense, just with a small subset of components larger than the rest. Furthermore, gradient sparsity varies during optimization, so methods assuming a fixed level of sparsity have limited practical use. Good methods need to explore the opportunity offered by sparse gradients when they are present and still work even when gradients are not sparse.

In this work, we propose a new method, which we coin ZORO, for high dimensional *regularized* zeroth-order optimization problems:

$$\underset{x \in \mathbb{R}^d}{\text{minimize}} F(x) := f(x) + r(x), \quad (3)$$

where $r(x)$ is an *explicit* proximable function that helps encode prior information about the solution. (We access $f(x)$ only implicitly through an oracle.) ZORO exploits both the exact sparse gradient assumption and a more flexible *compressibility* assumption. Moreover, ZORO employs a novel *adaptive sampling* strategy for improved gradient estimation. ZORO can converge even if the approximations to true gradients, sparse or not, are very loose. In addition, both noise-free oracles and *adversarially noisy* oracles are studied. Comprehensive analyses are provided for the proposed method under different settings.

1.1 Related work, contributions, and notation

Arguably, the first methods to employ zeroth order gradient estimators within a gradient-based optimization method are FDSA (Kiefer et al., 1952) and SPSA (Spall, 1998). SPSA was comprehensively analyzed in (Nesterov & Spokoiny, 2011)¹ where it was shown that after T oracle queries, $f(x_T) - \min f \leq O(d/T)$ for noise-free oracles, and $\mathbb{E}[f(x_T) - \min f] \leq O(d/\sqrt{T})$ for stochastic oracles with unspecified dependence on the stochasticity: $E_f(x) = F(x, \xi)$, but satisfying $\mathbb{E}[F(x, \xi)] = f(x)$. This convergence rate was improved to $O(\sqrt{d/T})$ in (Ghadimi & Lan, 2013), and this rate is also achieved in (Lian et al., 2016). In (Jamieson et al., 2012), it is shown that for strongly convex $f(x)$ and oracle of the form (2) with zero-mean noise, the zeroth order optimization problem is in $\Omega(\sqrt{d/T})$. Thus, the rate achieved in (Ghadimi & Lan, 2013; Lian et al., 2016) is essentially optimal without placing further assumptions on $f(x)$.

(Wang et al., 2018) first proposed the exact sparse gradient assumption, as well as a gradient estimator exploiting the assumption. Using this estimator in a mirror descent scheme and assuming zero-mean oracle noise, a convergence rate of $O((s/T)^{1/3} \log(d))$ was shown, where $\|\nabla f(x)\|_0 \leq s$ for all x . The sparse gradient assumption was also used in (Balasubramanian & Ghadimi, 2018), where a projected gradient descent scheme using carefully chosen step sizes was advertised as achieving a convergence rate of $O((s/T)^{1/2} \log(d))$. However, their analysis implicitly requires that the support of $\nabla f(x)$ is *fixed*, which is a more stringent requirement than an uniform bound on the sparsity of gradients.

We also mention several recent papers (Liu et al., 2018, 2019; Chen et al., 2019), which propose zeroth-order versions of ADMM, signSGD and Adam, respectively. Finally, for a comprehensive overview of zeroth-order optimization methods, we refer the interested readers to the recent survey article (Larson et al., 2019).

Contributions: The main innovations of this paper are:

- (i) We extend the assumption of exact gradient sparsity to *gradient compressibility*, and provide improved query complexity bounds for the noise-free oracle case (see Corollary 5.2). We do *not* assume the support of large nonzero entries remain the same across iterations.
- (ii) We introduce the notion of restricted strong convexity to zeroth-order optimization, and show that under this assumption, ZORO achieves *linear convergence* in the noise-free case with *adaptive query radius* (see Corollary 5.2).
- (iii) We study *regularized* zeroth-order optimization (See (3)). To the best of our knowledge, the only other paper to consider this problem is (Liu et al., 2018), but here we combine regularization with gradient sparsity which presents some interesting challenges.
- (iv) We consider *adversarial* (i.e., bounded but arbitrary) oracle noise. This is a different paradigm to the stochastic noise considered in (Wang et al., 2018; Balasubramanian & Ghadimi, 2018); hence our convergence results have a different flavor. Specifically, we show $O(s \log(d)/T)$ convergence to a certain error horizon, beyond which no further decrease in objective function value is possible (see Corollary 5.8, part 1). When $f(x)$ is restricted strongly convex, we improve this to a *linear convergence* rate, again up until a certain error horizon (see Corollary 5.8, part 2).

¹This later appeared as (Nesterov & Spokoiny, 2017).

- (v) To make our algorithm more practical, we develop a novel *adaptive sampling* strategy that exploits approximate gradient sparsity when it is present and still works if it is not. If all sampled gradients are compressible, the above sample complexities remain valid; otherwise, the strategy takes around d samples in each step and has a complexity no worse than those of existing methods.
- (vi) Finally, we successfully apply ZORO to some real-world applications, for example asset risk management (see Section 6.2) and sparse adversarial attacks on ImageNet (see Section 6.3). In contrast, previous works on zeroth-order optimization with sparse gradients have provided numerical results on synthetic datasets only.

Notation: For any vector or matrix, $\|\cdot\|_0$ counts the non-zero entries; $\|\cdot\|_1$ and $\|\cdot\|_2$ denote the entrywise ℓ_1 -norm and ℓ_2 -norm, respectively. The gradient and Hessian of function f are denoted by ∇f and $\nabla^2 f$, respectively. We shall frequently use $\mathbf{g} := \nabla f(x)$ when the point, x , in question is clear. For ease of presentation, we also write $\min F := \min\{F(x) : x \in \mathbb{R}^d\}$ and $e_k := F(x_k) - \min F$, where x_k is the k -th iteration point of ZORO. Moreover, $[x]_{(s)}$ denotes the best s -sparse approximation to vector x while $|x|_{(i)}$ denotes the i -th largest-in-magnitude component of x . It will be useful to define the indicator function:

$$1_{\text{ncvx}} = \begin{cases} 1 & \text{if } r(x) \text{ is non-convex,} \\ 0 & \text{otherwise.} \end{cases}$$

2 Problem setup

Firstly, we present the assumptions on the sparse gradients.

Assumption 1 (Sparse gradients). We consider three types of sparsity for the gradients:

1.a (Exact sparsity). The gradients of f are *exactly s -sparse* if $\|\nabla f(x)\|_0 \leq s_{\text{exact}}$ for all $x \in \mathbb{R}^d$.

1.b (Compressibility). The gradients of f are *compressible* if there exists a $p \in (0, 1)$ such that $|\nabla f(x)|_{(i)} \leq \|\nabla f(x)\|_2 i^{-1/p}$.

Assumption 1.a is standard in the prior literature (Wang et al., 2018; Balasubramanian & Ghadimi, 2018). Assumption 1.b does not explicitly specify support size s . However, one can easily show that it implies

$$\|\nabla f(x) - [\nabla f(x)]_{(s)}\|_1 \leq \left(\frac{1}{p} - 1\right)^{-1} \|\nabla f(x)\|_2 s^{1-1/p} \quad (4)$$

$$\|\nabla f(x) - [\nabla f(x)]_{(s)}\|_2 \leq \left(\frac{2}{p} - 1\right)^{-1/2} \|\nabla f(x)\|_2 s^{1/2-1/p}; \quad (5)$$

see, for example, (Needell & Tropp, 2009, Section 2.5). Hence one can choose s such that $\|\nabla f(x) - [\nabla f(x)]_{(s)}\|_2 \leq \psi \|\nabla f(x)\|_2$ where ψ is some small numerical constant. We also make the following assumption on the Hessian matrix of f , which is needed *only* when the oracle is noisy.

Assumption 2 (Bounded Hessian). Let f be twice differentiable. Then there exists a constant H such that $\|\nabla^2 f(x)\|_1 \leq H$ for all $x \in \mathbb{R}^d$.

This assumption also appears in Wang et al. (2018). Next, we present a standard assumption on the existence of minimizers of F and the smoothness of f .

Assumption 3 (Non-empty solution set and Lipschitz continuous gradients). (i) The solution set of F is non-empty. (ii) For any $x, y \in \mathbb{R}^d$, we have that $\|\nabla f(x) - \nabla f(y)\|_2 \leq L\|x - y\|_2$ for some constant L .

We emphasize that we are not assuming that we have access to ∇f , only that the Lipschitz property holds for ∇f . Next, we present the assumption on our noise model.

Assumption 4 (Adversarially noisy oracle). The oracle noise ξ is bounded: $\|\xi\|_2 \leq \sigma$.

We do not assume the noise is zero-mean; nor do we assume its probability distribution is known.

Our analysis considers several different settings of regularized objective function F , involving convex and restricted strongly convex components. We provide the definitions of convexity and restricted strongly convexity and coercivity. We also provide an extended notion of proximal operator.

Definition 1 (Convexity). A function h is *convex* if

$$h(tx + (1-t)y) \leq th(x) + (1-t)h(y) \quad (6)$$

for all $x, y \in \mathbb{R}^d$ and $t \in [0, 1]$. Additionally, if h is differentiable, then (6) is equivalent to

$$h(y) \geq h(x) + \nabla h(x)^\top (y - x) \quad (7)$$

for all $x, y \in \mathbb{R}^d$.

Definition 2 (Restricted strong convexity). A function h is *restricted ν -strongly convex* if

$$h(x) - \min h \geq \nu\|x - P_*(x)\|_2^2 \quad (8)$$

for all $x \in \mathbb{R}^d$, where $P_*(\cdot)$ is a projection operator onto the solution set defined by $P_*(x) := \operatorname{argmin}_{y \in \text{solution set of } h} \|y - x\|_2$.

One can see Definition 2 is indeed weaker than the commonly used strong convexity. We refer the interested readers to (Schöpfer, 2016; Zhang, 2017) for more results.

Definition 3 (Coercivity). 1. A function $h : \mathbb{R}^d \rightarrow \mathbb{R}$ is *coercive* if $\lim_{\|x\|_2 \rightarrow \infty} h(x) = +\infty$.

2. More generally, a function $h : \mathbb{R}^d \rightarrow \mathbb{R}$ is *coercive with respect to $g : \mathbb{R}^d \rightarrow \mathbb{R}$* if for any $\{x_k\}_{k=1}^\infty$ satisfying $\lim_{k \rightarrow \infty} g(x_k) = +\infty$ we also have $\lim_{k \rightarrow \infty} h(x_k) = +\infty$.

3. Finally, a set-valued operator A on \mathbb{R}^d is coercive with respect to $g : \mathbb{R}^d \rightarrow \mathbb{R}$ if for any $\{x_k\}_{k=1}^\infty$ satisfying $\lim_{k \rightarrow \infty} g(x_k) = +\infty$ we also have that $\lim_{k \rightarrow \infty} \inf_{y \in A(x_k)} \|y\|_2 = +\infty$.

If $r(x)$ is closed proper convex then

$$\mathbf{prox}_{\alpha r}(y) := \operatorname{argmin}_{x \in \mathbb{R}^d} r(x) + \frac{1}{2\alpha} \|x - y\|_2^2. \quad (9)$$

is well-defined. More generally:

Definition 4 (Proximability). $r(x)$ is *proximable* if $\mathbf{prox}_{\alpha r}(y)$, as defined in (9), is a single-valued operator.

Algorithm 1 Zeroth Order Regularized Optimization Method (ZORO)

- 1: **Input:** x_0 : initial point; s : gradient sparsity level; α : step size; β : query radius parameter; δ_0 : initial query radius, ϕ (*optional*): error tolerance for OppGradEst.
- 2: $m \leftarrow b_1 s \log(d/s)$ where b_1 is as in Lemma A.1. Typically $b_1 \approx 4$ is appropriate
- 3: **for** $i = 1$ **to** m **do**
- 4: Generate Rademacher random vector z_i .
- 5: **end for**
- 6: **for** $k = 0$ **to** K **do**
- 7: $\begin{cases} \hat{\mathbf{g}}_k \leftarrow \text{GradientEstimation}(x_k, s, \delta_k, \{z_i\}_{i=1}^m) & \text{or,} \\ (\hat{\mathbf{g}}_k, \{z_i\}_{i=1}^m) \leftarrow \text{OppGradEst}(x_k, \hat{S}_{k-1}, \delta_k, \{z_i\}_{i=1}^m, \phi) \end{cases}$
- 8: $x_{k+1} \leftarrow \mathbf{prox}_{\alpha r}(x_k - \alpha \hat{\mathbf{g}}_k)$
- 9: $\delta_{k+1} \leftarrow \begin{cases} \beta \|\hat{\mathbf{g}}_k\|_2 & \text{Noise-free oracle case and } r(x) = 0 \\ 1/k^{1.1} & \text{Noise-free oracle and } r(x) \neq 0 \\ \sqrt{2\sigma/H} & \text{Noisy oracle case} \end{cases}$
- 10: $\hat{S}_k \leftarrow \text{supp}(\hat{\mathbf{g}}_k)$
- 11: **end for**
- 12: **Output:** x_K : minimizer of (3).

3 Proposed method

In this section, we present the proposed novel method for solving regularized minimization problem (3), coined Zeroth-Order Regularized Optimization (ZORO). Proximal-gradient methods are a popular and well studied class of algorithms for structured optimization problems such as (3). To handle the potential non-smoothness of the regularizer, $r(x)$, we apply gradient descent with the estimated gradient, and then employ the proximal operator of $r(x)$. Hence each new iterate of ZORO is obtained as:

$$x_{k+1} = \mathbf{prox}_{\alpha r}(x_k - \alpha \hat{\mathbf{g}}_k).$$

When we estimate the gradient, different query radii are appropriate for the noise-free and noisy oracle cases. In either case, our query radius strategy ensures overall good sampling quality by tuning only one parameter. In summary, ZORO is proximal-gradient descent with an exact proximal operator but inexact gradients, estimated from zeroth-order information. We formalize ZORO as Method 1, and its convergence will be analyzed in Section 5 under different settings.

3.1 Gradient estimation

In this section we show how the compressible gradient estimation problem can be posed as a sparse recovery problem. Specifically, choose a query number m and a sampling radius δ , and let $\{z_i\}_{i=1}^m \in \mathbb{R}^d$ be Rademacher random vectors. That is:

$$(z_i)_j = \begin{cases} +1 & \text{with probability } 1/2, \\ -1 & \text{with probability } 1/2, \end{cases} \quad (10)$$

for all $i = 1, \dots, m$ and $j = 1, \dots, d$. (Gaussian and certain other types of random vectors will work, too. For space reasons, we investigate only the Rademacher type.) To construct each measurement

(in the compressed sensing sense) we make two oracle queries, at x and at $x + \delta z_i$, to obtain $E_f(x)$ and $E_f(x + \delta z_i)$. Then the measurements can be defined as

$$y_i = \frac{1}{\sqrt{m}} \frac{E_f(x + \delta z_i) - E_f(x)}{\delta}. \quad (11)$$

which are (noisy) finite difference approximations to the directional derivative in the directions z_i (divided by \sqrt{m}). We present this sampling procedure as Algorithm 2.

The next lemma characterizes measurements and their qualities.

Lemma 3.1. *If Assumptions 2 and 4 are satisfied, then*

$$y_i = \frac{1}{\sqrt{m}} z_i^\top \mathbf{g} + \frac{\mu_i}{\delta} + \delta \nu_i$$

with $\mathbf{g} = \nabla f(x)$, $|\mu_i| \leq 2\sigma/\sqrt{m}$, and $|\nu_i| \leq H/(2\sqrt{m})$.

Thus, if $f(x)$ also satisfies Assumption 1, one might hope to approximate \mathbf{g} via:

$$\hat{\mathbf{g}} = \underset{\mathbf{v} \in \mathbb{R}^d}{\operatorname{argmin}} \|Z\mathbf{v} - \mathbf{y}\|_2 \quad \text{such that } \|\mathbf{v}\|_0 \leq s, \quad (12)$$

where $\mathbf{y} = [y_1, \dots, y_m]^\top$ and $Z \in \mathbb{R}^{m \times d}$ is the *sensing matrix* whose i -th row is $\frac{1}{\sqrt{m}} z_i^\top$. We propose to solve Problem (12) approximately using CoSaMP (Needell & Tropp, 2009), and present the resulting gradient estimation procedure as Algorithm 3. In Theorem 3.2, we shall analyze the accuracy of this approach. Before proceeding, let us mention that an alternate approach to (12) could be to use LASSO:

$$\hat{\mathbf{g}} = \underset{\mathbf{v} \in \mathbb{R}^d}{\operatorname{argmin}} \frac{1}{2} \|Z\mathbf{v} - \mathbf{y}\|_2^2 + \lambda \|\mathbf{v}\|_1, \quad (13)$$

which is similar to the approach taken in (Wang et al., 2018). However, there are at least three reasons why a greedy approach such as CoSaMP could be preferable:

- (i) The LASSO estimator is typically biased (Fan & Li, 2001), while the CoSaMP estimator does not have this problem. This makes CoSaMP more appropriate for the compressible gradients case, and allows one to take (a constant factor) fewer oracle queries in the exactly sparse gradients case. Moreover, our analysis using CoSaMP allows for *adversarial noise*.
- (ii) CoSaMP is typically faster for small sparsity levels, s .
- (iii) Empirically, we have found that hand tuning LASSO's parameter λ is inefficient and it needs to be done dynamically to ensure convergence of main method (See Section 6).

The next theorem relates the quality of the estimated gradient $\hat{\mathbf{g}}$ to \mathbf{g} and parameters.

Theorem 3.2. *Suppose that $\{z_i\}_{i=1}^m$ are generated as described in Algorithm 1. Suppose further that Assumptions 1, 2 and 4 are satisfied. Then with probability at least $1 - (s/d)^{b_2 s}$:*

$$\|\hat{\mathbf{g}} - \mathbf{g}\|_2 \leq (\psi + \rho^n) \|\mathbf{g}\|_2 + \frac{2\tau\sigma}{\delta} + \frac{\tau\delta H}{2},$$

Algorithm 2 Sample

- 1: **Input:** x : current point; δ : query radius; r , $\{z_i\}_{i=1}^r$: sample number and directions.
- 2: Sample at point x , obtain $E_f(x)$.
- 3: **for** $i = 1$ **to** r **do**
- 4: Sample at point $x + \delta z_i$ to obtain $E_f(x + \delta z_i)$.
- 5: $y_i \leftarrow \frac{E_f(x + \delta z_i) - E_f(x)}{\delta}$
- 6: **end for**
- 7: $\mathbf{y} \leftarrow [y_1, \dots, y_r]^\top$
- 8: **Output:** \mathbf{y}

Algorithm 3 Gradient Estimation

- 1: **Input:** x : current point; s : gradient sparsity level as in Assumption 1.b; δ : query radius; $\{z_i\}_{i=1}^m$: sample directions.
- 2: $\mathbf{y} \leftarrow \frac{1}{\sqrt{m}} \text{Sample}(x, \delta, \{z_i\}_{i=1}^m)$
- 3: $Z \leftarrow \frac{1}{\sqrt{m}} [z_1, \dots, z_m]^\top$
- 4: $\hat{\mathbf{g}} \approx \underset{\|\mathbf{g}\|_0 \leq s}{\text{argmin}} \|Z\mathbf{g} - \mathbf{y}\|_2$ by CoSaMP
- 5: **Output:** $\hat{\mathbf{g}}$

for all $x \in \mathbb{R}^d$, where $\hat{\mathbf{g}}$ denotes the output after n iterations of CoSaMP applied to problem (12) and b_2 is defined as in Lemma A.1. Here $\rho < 1$ and $\tau \approx 15$ are fixed numerical constants, and:

$$\psi = \begin{cases} 0 & \text{if } f(x) \text{ satisfies Assumption 1.a,} \\ Cs^{1/2-1/p} & \text{if } f(x) \text{ satisfies Assumption 1.b.} \end{cases}$$

Note that C depends on p and $\{z_i\}_{i=1}^m$, but not on s .

The proofs of Lemma 3.1 and Theorem 3.2 can be found in Appendix A. The exact values of ρ and τ are given in (Foucart, 2012), while the exact form of C is given in Lemma A.5. Note that as $p \in (0, 1)$ we can make ψ (almost) arbitrarily small by taking s to be larger. We point out that the error bound in Theorem 3.2 is universal, *i.e.* it holds for all x with probability $1 - (s/d)^{b_2 s}$ where b_2 is defined as in Lemma A.1, and this probability is over the random draw of the $\{z_i\}_{i=1}^m$.

3.2 Opportunistic Sampling

To establish the convergence analysis for ZORO, we assume an uniform s for all $x \in \mathbb{R}^d$ in Assumption 1. Moreover, we assume no relationship between the support of the gradient at x_k , *i.e.* $\text{supp}(\mathbf{g}_k)$, and $\text{supp}(\mathbf{g}_{k+1})$. In practice, neither of these need to hold. The number of significant gradient coordinates can change—in particular, it tends to increase as $x_k \rightarrow x_*$ and $g_k \rightarrow 0$. Moreover, $\text{supp}(\mathbf{g}_k) \approx \text{supp}(\mathbf{g}_{k-1})$ holds at times, and they may even be equal. Hence, we can make two modifications to Algorithm 3 to take advantage of these phenomena, when they arise. We present this as Algorithm 4. Informally, Algorithm 4 proceeds as:

1. First, we test if $\text{supp}(\mathbf{g}_k) \subseteq \text{supp}(\mathbf{g}_{k-1})$. We do this by taking only s samples and solving a least squares problem with support restricted to $\text{supp}(\mathbf{g}_{k-1})$ (see lines 2–4 of Algorithm 4). If the relative error in this solution is small, we immediately return this solution as $\hat{\mathbf{g}}_k$.

Algorithm 4 Opportunistic Gradient Estimation (OppGradEst)

```

1: Input:  $x$ : current point;  $\hat{S}_{k-1}$ : support of  $\hat{\mathbf{g}}_{k-1}$ ;  $\delta$ : query radius;  $\{z_i\}_{i=1}^m$ : sample directions;
    $\phi$ : error tolerance.
2:  $s \leftarrow |\hat{S}_{k-1}|$ 
3:  $\mathbf{y} \leftarrow \text{Sample}(x, \delta, \{z_i\}_{i=1}^s)$ 
4:  $Z \leftarrow [z_1, \dots, z_s]^\top$ 
5:  $\hat{\mathbf{g}} \leftarrow \operatorname{argmin}_{\mathbf{g}} \|Z\mathbf{g} - \mathbf{y}\|_2 \text{ s.t. } \text{supp}(\mathbf{g}) = \hat{S}_{k-1}$ 
6: if  $\|Z\hat{\mathbf{g}} - \mathbf{y}\|_2/\|\mathbf{y}\|_2 \leq \phi$  then
7:   Terminate algorithm and output
8: end if
9:  $\mathbf{y} \leftarrow \frac{1}{\sqrt{m}}[\mathbf{y}; \text{Sample}(x, \delta, \{z_i\}_{i=s+1}^m)]$ 
10:  $Z \leftarrow \frac{1}{\sqrt{m}}[z_1, \dots, z_m]^\top$ 
11:  $\hat{\mathbf{g}} \approx \operatorname{argmin}_{\|\mathbf{g}\|_0 \leq s} \|Z\mathbf{g} - \mathbf{y}\|_2 \text{ by CoSaMP}$ 
12: while  $\|Z\hat{\mathbf{g}} - \mathbf{y}\|_2/\|\mathbf{y}\|_2 > \phi$  do
13:    $m^{\text{new}} \leftarrow m + \log(d/s)$ 
14:   Generate Rademacher random vectors  $z_{m+1}, \dots, z_{m^{\text{new}}}$ 
15:    $\mathbf{y} \leftarrow \frac{1}{\sqrt{m^{\text{new}}}}[\sqrt{m}\mathbf{y}; \text{Sample}(x, \delta, \{z_i\}_{i=m+1}^{m^{\text{new}}})]$ 
16:    $Z \leftarrow \frac{1}{\sqrt{m^{\text{new}}}}[\sqrt{m}Z^\top, z_{m+1}, \dots, z_{m^{\text{new}}}]^\top$ 
17:    $m \leftarrow m^{\text{new}}$  and  $s \leftarrow s + 1$ 
18:    $\hat{\mathbf{g}} \approx \operatorname{argmin}_{\|\mathbf{g}\|_0 \leq s} \|Z\mathbf{g} - \mathbf{y}\|_2 \text{ by CoSaMP}$ 
19: end while
20: Output:  $\hat{\mathbf{g}}, \{z_i\}_{i=1}^m$ 

```

2. If Algorithm 4 does not terminate after the above, we run a variation of Gradient Estimation (see lines 8–10 of Algorithm 4) while reusing the s samples we have already taken. We check whether the solution arising from this is sufficiently accurate (line 12 of Algorithm 4).
3. Until a sufficiently accurate solution is found, we generate additional z_i and oracle queries $E_f(x + \delta z_i)$, while retaining our earlier samples. We estimate the gradient from these samples, old and new, (see lines 13–18 of Algorithm 4) and check whether it is sufficiently accurate.

At worst, we make around d queries, which is no worse than the dense gradient estimators. In our tests, d queries were never needed though. For example, in the asset allocation experiment below, the gradients have 225 entries and are dense, but it is enough for ZORO to use sparse approximate gradients (with only 40 to 72 nonzeros) to converge. Nevertheless, the adaptive strategy provides us a safeguard even if the gradients become completely dense and non-compressible.

4 Inexact (proximal-) gradient descent

Recall the sequence produced by ZORO can be written as:

$$x_{k+1} = \mathbf{prox}_{\alpha r}(x_k - \alpha \hat{\mathbf{g}}_k). \quad (14)$$

Note that if $r(x) = 0$ (*i.e.*, there is no regularization), then (14) reduces to (inexact) gradient descent: $x_{k+1} = x_k - \alpha \hat{\mathbf{g}}_k$. In the case where $r(x) \neq 0$ we may write:

$$x_{k+1} = x_k - \alpha \underbrace{(\tilde{\nabla}r(x_{k+1}) + \hat{\mathbf{g}}_k)}_{-\hat{\Delta}_k}, \quad (15)$$

where $\tilde{\nabla}r(x_{k+1}) = \frac{1}{\alpha}((x_k - \alpha\hat{g}_k) - \mathbf{prox}_{\alpha r}(x_k - \alpha\hat{g}_k)) \in \partial r(x_{k+1})$ is the subgradient picked out by the proximal operator. Moreover, we define

$$\begin{aligned} \text{Actual direction:} \quad & \hat{\Delta}_k := -(\tilde{\nabla}r(x_{k+1}) + \hat{\mathbf{g}}_k), \\ \text{Ideal direction:} \quad & \Delta_k := -(\tilde{\nabla}r(x_{k+1}) + \mathbf{g}_k), \\ \text{Stationarity:} \quad & \tilde{\Delta}_k := -(\tilde{\nabla}r(x_{k+1}) + \mathbf{g}_{k+1}). \end{aligned}$$

Note $\hat{\Delta}_k = \frac{1}{\alpha}(x_{k+1} - x_k)$. The three quantities have the following relations:

$$|\|\hat{\Delta}_k\|_2 - \|\Delta_k\|_2| \leq \|\hat{\mathbf{g}}_k - \mathbf{g}_k\|_2, \quad (16)$$

$$|\|\tilde{\Delta}_k\|_2 - \|\Delta_k\|_2| \leq \|\mathbf{g}_{k+1} - \mathbf{g}_k\|_2 \leq \alpha L \|\hat{\Delta}_k\|_2. \quad (17)$$

In this and next section, the constant R , as in $\|x_k - \mathbf{P}_*(x_k)\|_2 \leq R$ for all k , denotes a number depending only on the coercivity of $f(x)$ and a growth condition described in Appendix B. We defer all proofs for this section to Appendix B.

Below we use

$$e_k = F(x_k) - \min F$$

as objective error. Other letters are summarized in the table in the Appendix.

4.1 Convex case

Here we assume that both $f(x)$ and $r(x)$ are convex. While there exist several results in the literature (see, for example, Theorem 2.2 in Friedlander & Schmidt (2012)) of the same flavor as Part 1 of Theorem 4.1, we believe Part 2 to be novel.

Theorem 4.1 (Sublinear convergence). *Suppose that $f(x)$ and $r(x)$ are convex and Assumption 3 is satisfied. If in addition:*

1. **Absolute bound**²: $\|\mathbf{g}_k - \hat{\mathbf{g}}_k\|_2 \leq \varepsilon_{\text{abs}}$, $\alpha < 2/L$ and $\|x_k - \mathbf{P}_*(x_k)\|_2 \leq R$ for $k = 1, \dots, K$, then:

$$\begin{aligned} e_K & \leq \max \left\{ \frac{e_0}{Ke_0/(c_7 R^2) + 2}, R\sqrt{c_8 \varepsilon_{\text{abs}}} \right\} \\ & \sim \max \left\{ c_7 R^2 \cdot \frac{1}{K}, R\sqrt{c_8 \varepsilon_{\text{abs}}} \right\}. \end{aligned}$$

2. **Relative bound**: $r(x) = 0$, $\|\mathbf{g}_k - \hat{\mathbf{g}}_k\|_2 \leq \varepsilon_{\text{rel}} \|\mathbf{g}_k\|_2$, $\alpha < 2/L$ and $\|x_k - \mathbf{P}_*(x_k)\|_2 \leq R$ for all k , then:

$$e_k \leq \frac{e_0}{ke_0/(c_9 R^2) + 1} \sim c_9 R^2 \cdot \frac{1}{k}.$$

²We use the symbol “ \sim ” to keep only the leading term in the polynomial.

The constants c_7 , c_8 and c_9 are defined as in Lemma B.5.

We remark that the assumption $\|x_k - P_*(x_k)\|_2 \leq R$ is rather strong. In Proposition B.6 we provide weaker sufficient conditions under which this holds.

4.2 Restricted strongly convex case

Here, we present some useful results on inexact gradient descent when $F(x)$ is restricted strongly convex. Note that part 1 of Theorem 4.2 extends Corollary 1 of (Zhang & Cheng, 2015) to inexact proximal-gradient descent.

Theorem 4.2 (Linear convergence). *Suppose that $F(x)$ is convex, restricted ν -strongly convex and satisfies Assumption 3. Suppose that $r(x)$ is proximable. If in addition:*

1. **Absolute bound:** $\|\mathbf{g}_k - \hat{\mathbf{g}}_k\|_2^2 \leq \varepsilon_{\text{abs}} \forall k$ and $\alpha < (2 - 1_{\text{ncvx}})/L$, then

$$e_k \leq c_{10}^k e_0 + (1 - c_{10})^{-1} c_{11} \varepsilon_{\text{abs}}$$

with constants $c_{10} = 1 - \nu\alpha^2 c_3$ and $c_{11} = c_4$ where c_3 and c_4 are defined as in Lemma B.3.

2. **Relative bound:** $r(x) = 0$, $\|\mathbf{g}_k - \hat{\mathbf{g}}_k\|_2 \leq \varepsilon_{\text{rel}} \|\mathbf{g}_k\|_2 \forall k$ and $\alpha < \frac{2(1 - \varepsilon_{\text{rel}}^2)}{L(1 + \varepsilon_{\text{rel}}^2)}$, then

$$e_k \leq c_{12}^k e_0$$

where $c_{12} = 1 - \frac{1}{4}\nu\alpha(2 - 2\varepsilon_{\text{rel}}^2 - \alpha L - \alpha L\varepsilon_{\text{rel}}^2) < 1$.

4.3 Non-convex case

Finally, we consider the case where $F(x)$ is non-convex.

Theorem 4.3. *Suppose that $F(x)$ satisfies Assumption 3 and $r(x)$ is proximable.*

1. **Square-summable noise:** Define $E_K^2 := \sum_{k=0}^K \|\hat{\mathbf{g}}_k - \mathbf{g}_k\|_2^2$. If $E_K^2 \leq E_\infty^2 < \infty$ for all K then:

$$\begin{aligned} \min_{1 \leq t \leq k} \|\Delta_t\|_2^2 &\leq \frac{1}{k+1} (c_5 e_0 + c_6 E_\infty^2), \\ \min_{1 \leq t \leq k} \|\hat{\Delta}_t\|_2^2 &\leq \frac{1}{k+1} (\hat{c}_5 e_0 + \hat{c}_6 E_\infty^2), \\ \min_{1 \leq t \leq k} \|\tilde{\Delta}_k\|_2^2 &\leq \frac{1}{k+1} (\tilde{c}_5 e_0 + \tilde{c}_6 E_\infty^2). \end{aligned}$$

2. **Non-summable noise:** assuming $\|\hat{\mathbf{g}}_k - \mathbf{g}_k\|_2^2 \leq \varepsilon_{\text{abs}}$ for all k , we get:

$$\begin{aligned} \min_{1 \leq t \leq k} \|\Delta_t\|_2^2 &\leq \frac{c_5}{k+1} e_0 + c_6 \varepsilon_{\text{abs}}, \\ \min_{1 \leq t \leq k} \|\hat{\Delta}_t\|_2^2 &\leq \frac{\hat{c}_5}{k+1} e_0 + \hat{c}_6 \varepsilon_{\text{abs}}, \\ \min_{1 \leq t \leq k} \|\tilde{\Delta}_k\|_2^2 &\leq \frac{\tilde{c}_5}{k+1} e_0 + \tilde{c}_6 \varepsilon_{\text{abs}}. \end{aligned}$$

The constants are defined as in Lemma B.4.

5 Convergence analysis for ZORO

In this section we present a variety of convergence results for ZORO, under different assumptions on $f(x)$, $r(x)$ and $E_f(x)$. For simplicity, in Sections 5.1 and 5.2 we shall assume ZORO is implemented using the simpler GradientEstimation Algorithm (Algorithm 3). We discuss how one might adapt these results to ZORO using OppGradEst (Algorithm 4) in Section 5.3.

5.1 Noise-free oracle case

Here, we assume that the oracle is noise-free, *i.e.* $\sigma = 0$ in Assumption 4. The main result of this section is that by choosing δ_k adaptively, one can guarantee that $\|\mathbf{g}_k - \hat{\mathbf{g}}_k\|_2 \leq \varepsilon_{\text{rel}} \|\mathbf{g}_k\|_2$ for all k , with high probability.

Theorem 5.1. *Suppose that $f(x)$ satisfies Assumption 1. If $f(x)$ satisfies Assumption 1.b then let s be chosen large enough such that $\psi < \min\left\{\frac{1-\alpha L}{2-\alpha L}, \frac{2-\alpha L}{4-\alpha L}\right\}$. Suppose further that $f(x)$ satisfies Assumption 3 and that $\alpha < 1/L$. Choose ε_{rel} and n such that:*

$$\psi + \rho^n < \varepsilon_{\text{rel}} < \min\left\{\frac{1-\alpha L}{2-\alpha L}, \frac{2-\alpha L}{4-\alpha L}\right\},$$

and define:

$$\beta = \frac{2(\varepsilon_{\text{rel}} - \psi - \rho^n)(1 - L\alpha - \varepsilon_{\text{rel}}(2 - \alpha L))}{\tau H(1 - \varepsilon_{\text{rel}})}.$$

If $\|\mathbf{g}_0 - \hat{\mathbf{g}}_0\|_2 \leq \varepsilon_{\text{rel}} \|\mathbf{g}_0\|_2$ and $\delta_k < \beta \|\hat{\mathbf{g}}_{k-1}\|_2$, then:

$$\|\mathbf{g}_k - \hat{\mathbf{g}}_k\|_2 \leq \varepsilon_{\text{rel}} \|\mathbf{g}_k\|_2$$

for all k with probability $1 - (s/d)^{b_2 s}$ where b_2 is defined as in Lemma A.1.

We defer the proofs of this section to Appendix C, where we also discuss how to guarantee that $\|\mathbf{g}_0 - \hat{\mathbf{g}}_0\|_2 \leq \varepsilon_{\text{rel}} \|\mathbf{g}_0\|_2$. The constant ψ is discussed in Theorem 3.2 and defined in Lemma A.5. Note that this, combined with the results of Section 4 immediately yield the following:

Corollary 5.2. *Assume the hypotheses of Theorem 5.1. Let $r(x) = 0$ and let x_K be the iterate returned by ZORO after making T oracle queries, where $K = T/m$.*

1. *If $f(x)$ is convex and coercive then:*

$$e_K \leq \frac{c_9 e_0 R^2}{T e_0 / b_1 s \log(d/s) + c_9 R^2} = O\left(\frac{s \log(d/s)}{T}\right),$$

with probability at least $1 - (s/d)^{b_2 s}$. The constants b_1 and b_2 are defined as in Lemma A.1.

2. *If $f(x)$ is convex and restricted ν -strongly convex then:*

$$e_K \leq e_0 c_{12}^{T/b_1 s \log(d/s)}$$

again with probability at least $1 - (s/d)^{b_2 s}$. Choosing step size $\alpha < \frac{2-2\varepsilon_{\text{rel}}^2}{L+L\varepsilon_{\text{rel}}^2}$ guarantees $c_{12} < 1$.

We now consider the case $r(x) \neq 0$.

Theorem 5.3. *Suppose that $f(x)$ satisfies Assumptions 1.a and 3. If $\delta_k < 1/k^{1.1}$ and n is sufficiently large, then*

$$\|\mathbf{g}_k - \hat{\mathbf{g}}_k\|_2 \leq \tau H/k^{1.1}$$

for all k , with probability at least $1 - (s/d)^{b_2 s}$.

In Appendix C we discuss exactly how large n should be.

Corollary 5.4. *Let $F(x) := f(x) + r(x)$ with $f(x)$ convex and satisfying Assumptions 1.a, 2 and 3 and $r(x)$ a closed proper convex function. Choose $\alpha = 1/L$ and let $\{x_1, \dots, x_K\}$ be the iterates found by ZORO after making T total oracle queries, where $K = T/m$. Then:*

$$\min_{k=1, \dots, K} F(x_i) - \min F \leq \frac{Ls \log(d/s)}{2T} \left(\|x_0 - P_*(x_0)\|_2 + \frac{2E_K^1}{L} \right).$$

with probability at least $1 - (s/d)^{b_2 s}$, where $E_K^1 = \sum_{k=1}^K \|\mathbf{g}_k - \hat{\mathbf{g}}_k\|_2$.

Note that

$$E_K^1 \leq \sum_{k=1}^{\infty} \|\mathbf{g}_k - \hat{\mathbf{g}}_k\|_2 \leq \tau H \sum_{k=1}^{\infty} k^{-1.1} =: E_{\infty}^1 < \infty$$

Remark 5.5. It is an interesting question whether one can extend Corollary 5.4 to allow for compressible, instead of sparse, gradients. We found the main obstacle to be extending Theorem 5.1 to a bound of the form $\|\mathbf{g}_k - \hat{\mathbf{g}}_k\|_2 \leq \varepsilon_{\text{rel}} \|\tilde{\Delta}_k\|_2$. We leave this line of enquiry for future research.

Finally we prove convergence to stationarity for non-convex $F(x)$.

Corollary 5.6. *Let $F(x) = f(x) + r(x)$ where $f(x)$ satisfies Assumption 3, $r(x)$ is proximable and $\alpha < 2/L$ if $r(x)$ is convex while $\alpha < 1/L$ if $r(x)$ is non-convex. Let $\{x_1, \dots, x_K\}$ be the iterates found by ZORO after making T oracle queries, where $K = T/m$. Then:*

$$\min_{k=1, \dots, K} \|\tilde{\Delta}_k\|_2 \leq \frac{1}{\sqrt{k+1}} (\tilde{c}_5 e_0 + \tilde{c}_6 E_{\infty}^2)^{1/2}$$

holds with probability at least $1 - (s/d)^{b_2 s}$, where $E_{\infty}^2 = \tau H \sum_{k=1}^{\infty} k^{-1.1}$

5.2 Noisy oracle case

Here we consider a noisy oracle, *i.e.* $\sigma > 0$ in Assumption 4. For ease of comparison with (Wang et al., 2018) we consider the exact sparsity case (*i.e.*, Assumption 1.a).

Theorem 5.7. *Suppose that $f(x)$ satisfies Assumptions 1.a, 2 and 3, $\delta_k = \delta = \sqrt{2\sigma/H}$ and n is sufficiently large. Then for all k :*

$$\|\hat{\mathbf{g}}_k - \mathbf{g}_k\|_2 \leq 2\sqrt{2\tau\sigma H}$$

with probability at least $1 - (s/d)^{b_2 s}$.

In Appendix C we quantify precisely how large n should be. Let us combine this with the estimates of Theorem 4.1.

Corollary 5.8. *Assume the hypotheses of Theorem 5.7 and suppose that, in addition, $f(x)$ and $r(x)$ are convex. Let x_K be the iterate returned by ZORO with $\alpha < 2/L$ after making T oracle queries, where $K = T/m$. Then:*

1. *If $F(x)$ is coercive and $\|\partial F(x)\|_2$ is coercive with respect to $f(x)$:*

$$\begin{aligned} e_K &\leq \max \left\{ \frac{c_7 e_0 R^2}{T e_0 / b_1 s \log(d/s) + 2c_7 R^2}, 2^{\frac{3}{4}} R c_8^{\frac{1}{2}} (\tau \sigma H)^{\frac{1}{4}} \right\} \\ &= O \left(\max \left\{ \frac{s \log(d/s)}{T}, R (\sigma H)^{\frac{1}{4}} \right\} \right). \end{aligned}$$

with probability $1 - (s/d)^{b_2 s}$.

2. *If $F(x)$ is restricted ν -strongly convex:*

$$e_K \leq c_{10}^{T/b_1 s \log(d/s)} + 2^{3/2} (1 - c_{10})^{-1} c_{11} (\tau \sigma H)^{1/2}.$$

again with probability $1 - (s/d)^{b_2 s}$.

We remark that the coercivity assumptions are necessary. Consider the following simple, one-dimensional, example. Let $f(x)$ be the Huber loss function:

$$f(x) = \begin{cases} \frac{1}{2} x^2 & \text{for } |x| \leq m \\ m(|x| - \frac{1}{2} m) & \text{otherwise} \end{cases}$$

while $r(x) = 0$ and $\sigma > m^2$. From Theorem 5.7 we get that, at worst:

$$\|\mathbf{g}_k - \hat{\mathbf{g}}_k\| \approx 2^{3/2} \tau^{1/2} m > 2m \geq 2\|\mathbf{g}_k\| \quad (\text{as } H = 1).$$

That is, for all k the noise can be chosen adversarially such that $\text{sign}(\hat{\mathbf{g}}_k) \neq \text{sign}(\mathbf{g}_k)$, hence the inexact gradient descent may diverge. We also consider convergence to (approximate) stationarity for non-convex $F(x)$:

Corollary 5.9. *Let $F(x) = f(x) + r(x)$ where $f(x)$ satisfies Assumption 3 and $r(x)$ is proximable. Choose $\alpha < 2/L$ if $r(x)$ is convex and $\alpha < 1/L$ if $r(x)$ is non-convex. Let $\{x_1, \dots, x_K\}$ be the iterates found by ZORO after making T oracle queries, where $K = T/m$. Then:*

$$\min_{k=1, \dots, K} \|\tilde{\Delta}_k\|_2 \leq \frac{\sqrt{\tilde{c}_5 e_0}}{\sqrt{k+1}} + 2^{3/4} \tilde{c}_6^{1/2} (\tau \sigma H)^{1/4}$$

with probability at least $1 - (s/d)^{b_2 s}$.

5.3 Fixed gradient support

As a final example, we consider the case where $\text{supp}(\nabla f(x)) = S$ for all $x \in \mathbb{R}^d$. We consider ZORO with Algorithm 4.

Theorem 5.10. Suppose that $f(x)$ is convex, coercive and satisfies Assumption 1.a. Suppose that $r(x) = 0$ and $\sigma = 0$. Choose $\alpha < 1/L$ and $\varepsilon_{\text{rel}} < \min \left\{ \frac{1-\alpha L}{2-\alpha L}, \frac{2-\alpha L}{4-\alpha L}, \min_{i:i \in S} |(g_0)_i|/\|g_0\|_2 \right\}$ and define:

$$\beta = \varepsilon_{\text{rel}} \left(\frac{1 - \alpha L - \varepsilon_{\text{rel}}(2 - \alpha L)}{1 - \varepsilon_{\text{rel}}} \right) \frac{2\varepsilon_{\text{inv}}}{sH}$$

Suppose that $\|g_0 - \hat{g}_0\|_2 \leq \varepsilon_{\text{rel}}\|g_0\|_2$. For $k = 1, \dots, K$, choose *OppGradEst* (Algorithm 4) in line 7 of *ZORO* (Algorithm 1) with $\phi > 0$, and let x_K be the iterate found by *ZORO* after making T oracle queries, where $K = T/s$. Then:

$$e_K \leq \frac{c_9 e_0 R^2}{T e_0 / b_1 s + c_9 R^2} = O\left(\frac{s}{T}\right)$$

with probability at least $1 - O(\varepsilon_{\text{inv}})$.

Theorem 5.10 is rather optimistic; in particular, it would be hard to guarantee ε_{rel} satisfies the required condition in practice. Nevertheless, it gives some indication of the best possible performance of *ZORO* with opportunistic gradient estimation. In reality, we expect the performance to be somewhere between this and the more pessimistic guarantees of Sections 5.1 and 5.2. We note that Theorem 5.10 requires $\|g_0 - \hat{g}_0\|_2 \leq \varepsilon_{\text{rel}}\|g_0\|_2$. In Appendix C, we discuss how to do this without making too many more queries.

6 Numerical experiments

In this section, we demonstrate the practical usefulness of our method and compare its performance with other gradient estimation methods. Considerable effort has been invested into developing *global* zeroth-order optimization methods for high dimensional problems, *e.g.*, REMBO (Wang et al., 2013). In this paper, we will not compare the performance of *ZORO* against any global zeroth order algorithms directly, due to their strong correlations with problem structures. Furthermore, for the fairness of the comparison, we only use Algorithm 3 for CoSaMP gradient estimations in this section, so *ZORO* does not gain extra advantage from the consistent gradient supports with opportunistic gradient estimation.

6.1 Synthetic example

We consider the problem of minimizing a quadratic function $f(x) = x^\top A x / 2$, where $A \in \mathbb{R}^{200 \times 200}$ is a diagonal matrix. We experiment with two cases: (a) exact sparse case where only 20 diagonal elements are non-zero randomly generated positive numbers; (b) compressible case where all diagonal elements are non-zero but the diagonal element values diminish exponentially with respect to the row/column indexes, *i.e.*, $A_{i,i} = e^{-\omega i}$ with $\omega > 0$.

In case (a), for CoSaMP and OMP, we use the sparsity level and number of samples according to the sparse structure of the objective function. We use the same number of samples for LASSO. We use an identical step size for all methods except SPSA, whose convergence is not robust with large step size in practice. We also tested a proximal operator to enforce non-negative values. The results are shown in Figure 1. Unsurprisingly, the FDSA-based approach has the slowest convergence rate because it over-samples in the redundant dimensions. CoSaMP with proximal operator requires

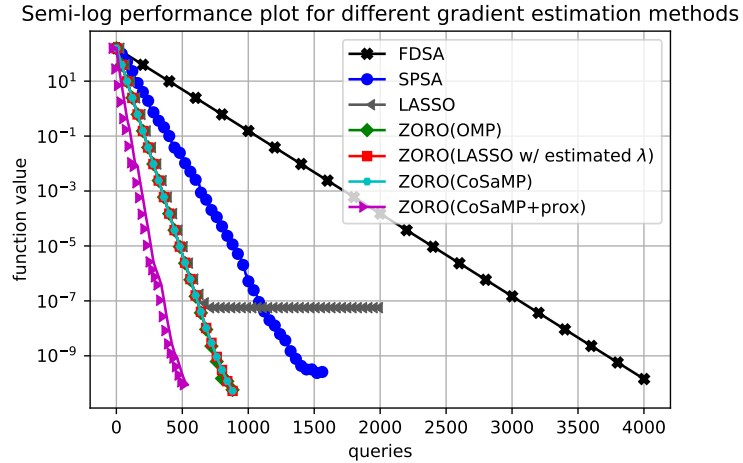


Figure 1: Function values *v.s.* queries comparisons between gradient estimation methods: exact sparse case.

about 50% fewer total queries as compared to other sparsity-aware methods that do not use a proximal operator.

Note that if we use a fixed regularizing parameter, λ , for LASSO then the function values stop decreasing after a large number of iterations. The reason for this is that the ratio between the ℓ_2 -norm squared term and the ℓ_1 term becomes too small to recover any non-zero gradient. To address this issue, we propose a numerical rule for estimating the regularizing parameter of LASSO. Specifically, at the $(k+1)$ -st iteration we use the ℓ_2 -norm square and ℓ_1 terms from the previous iteration to estimate the new parameter: $\lambda_{k+1} = c\|\mathbf{y}_k - Z_k \hat{\mathbf{g}}_k\|_2^2 / \|\hat{\mathbf{g}}_k\|_1$. Here c is a fixed parameter throughout the optimisation, and \mathbf{y}_k , Z_k and $\hat{\mathbf{g}}_k$ are as in Section 3.1. With this one-tap delay trick, ZORO with LASSO converges at the same speed as ZORO with other sparse coding methods, in terms of query complexity.

We further investigate the running time differences among three sparse coding methods, by recording 30 iterations of gradient descent. We compare their speeds under different dimensions and sparsity levels, which are summarized as Figures 5 and 6 in Appendix D. We find the greedy methods, CoSaMP and OMP, have a speed advantage when the problem dimension, d , is large and sparsity level, s , is small. Conversely, LASSO solvers are faster when both d and s are moderately sized. We emphasize that the gradients estimated by these three methods offer almost identical convergence performance on the easier synthetic tasks, so stop criteria will not affect our observation in this experiment.

We now discuss case (b), where we use a decay factor $\omega = 0.5$. The main challenge here is that the approximate sparsity level changes (mostly grows) over iterations. We add the simulation of the adaptive strategy described in Section 3.2 to handle this issue. We include the simulation of applying the adaptive strategy and the proximal operator, which converges the fastest among all methods. To demonstrate the effect of adaptive strategy, we plot the sparsity levels used at different iterations. All the simulation results are shown in Figure 2.

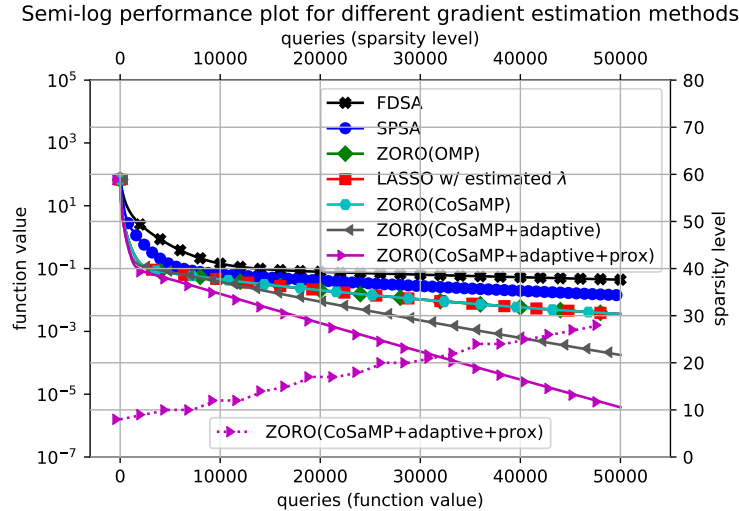


Figure 2: Function values *v.s.* queries comparisons between gradient estimation methods: approximately sparse case.

6.2 Asset risk management

We consider risk minimization problem for asset management. Suppose that a portfolio consists of n different assets. Let x_i denote the fraction of the portfolio invested in asset i . The rate of return of asset i is a random variable with expected value m_i . We use \mathcal{C} to denote the covariance matrix of asset returns. The portfolio risk, which we aim to minimize, can be written as $\frac{x^\top \mathcal{C} x}{2(\sum_{i=1}^n x_i)^2}$. Specifically for our experiments, we use the correlation, mean, and standard deviation of 225 assets from the dataset of (Chang et al., 2000). Our goal is to minimize the risk function given that the expected return should be no less than a minimal rate of portfolio return that the investor desires, *i.e.* $\frac{\sum_{i=1}^n m_i x_i}{\sum_{i=1}^n x_i} > r$. We add a penalty term to the risk function to describe the minimal rate return constraint and formulate the problem as follows:

$$\underset{x \in \mathbb{R}^d}{\text{minimize}} \frac{x^\top \mathcal{C} x}{2(\sum_{i=1}^n x_i)^2} + \lambda \left(\min \left\{ \frac{\sum_{i=1}^n m_i x_i}{\sum_{i=1}^n x_i} - r, 0 \right\} \right)^2.$$

If the optimizer has access to all the parameters, then it is natural to use quadratic programming to minimize the risk function. We are interested in cases where the optimizer can only access the objective function values. A natural benefit of such setting is that the optimizer has no access to the model or associated data and provides service in a “federated” fashion (*e.g.*, SigOPT).

We first experiment with the case where no constraints are applied on the allocation vector, *i.e.*, x_i can be negative. In other words, for each asset, the final portfolio can be either long or short on this asset. We use a fixed sparsity level and number of samples for this experiment. We use an identical randomly-generated initial point for all experiments. We have tuned the parameters for different sparse recovery methods to achieve their best convergence speeds. The results are shown in Figure 3. Note that CoSaMP has the best convergence rate among all methods. The final risks

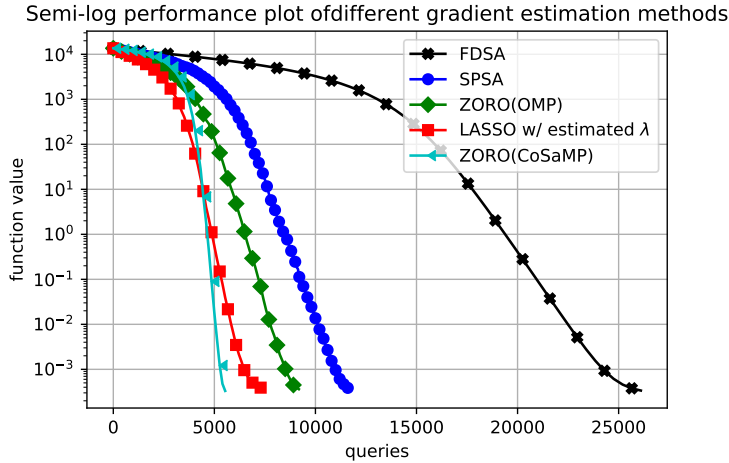


Figure 3: Function values *v.s.* queries comparisons between gradient estimation methods.

of all the methods are approximately 2×10^{-4} , which is consistent with the optimal risk using quadratic programming.

We now consider the long-only solution, *i.e.*, $x_i \geq 0$ for all i . To handle the constraints, we apply the following proximal operators after each gradient descent iteration:

$$x_i = x_i + \left| \min\{0, \min_{j=1,\dots,n} x_j\} \right|, \quad \forall i,$$

$$x_i = x_i / \sum_{j=1}^n x_j, \quad \forall i.$$

The first update shifts the variables based on the smallest negative variable (if any) to satisfy the long-only constraint. The second update projects an allocation in amount to an allocation in fractions. Here we implemented the adaptive strategy for both CoSaMP and OMP. The results are shown in Figure 4. Note that for SPSA, we are unable to obtain a set of parameters for stable convergence; partially due to the sensitivity to the step size along with proximal operator. FDSA converges to the optimum but is the least query-efficient. Gradient estimate methods with LASSO, OMP, and CoSaMP converge using carefully tuned hyper-parameters. We also find that the step size for CoSaMP gradient update can be more aggressive than those of LASSO and OMP, which leads to its out-performance. Comparing with the non-regularized case, the query complexities are significantly reduced for all methods with proximal operator and adaptive strategy.

6.3 Sparse adversarial attack on ImageNet

We consider the problem of generating black-box adversarial examples using zeroth-order optimization methods. We use Inception-V3 model (Szegedy et al., 2016) on ImageNet (Deng et al., 2009) and focus on the per-image adversarial attack problem. The authors in (Chen et al., 2019) considered a similar problem by optimizing the attack loss and the ℓ_2 -norm of image distortion. In contrast, we aim to design a distortion δ for a single image x such that the attack loss $f(x + \delta)$ and

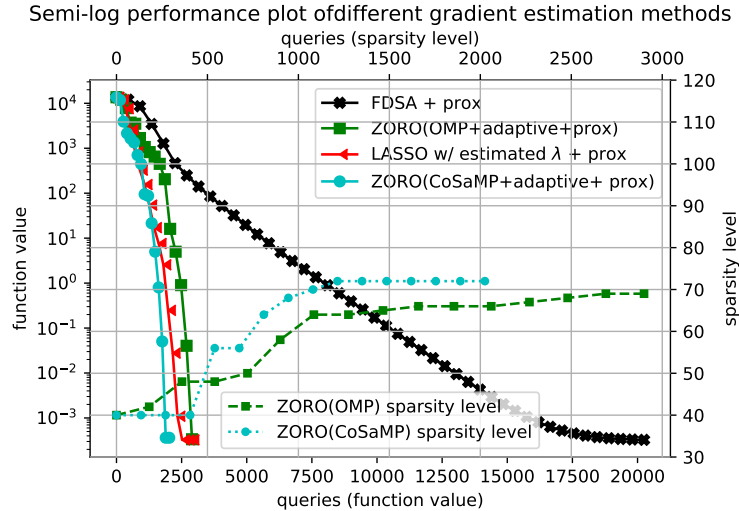


Figure 4: Function values *v.s.* queries comparisons between gradient estimation methods.

the ℓ_0 norm of distortion are minimized: $\text{minimize}_\delta f(x + \delta) + \lambda \|\delta\|_0$. Note that all the methods in (Chen et al., 2019) lead to extremely large ℓ_0 distortion norm, except ZO-SCD, which has the worse ℓ_2 distortion norm. In other words, successful attacks require distorting almost all of the pixels. We compare ZORO with ZO-AdaMM, ZO-SGD, and ZO-SCD (Chen et al., 2019). Note that ZO-SCD is essentially a variation of FDSA and ZO-SGD is a mini-batched version of SPSA. For these methods, we use the same experimental setup as (Chen et al., 2019), which uses 10 queries at each iteration and determines if the attack successes before 1000 iterations. For ZORO, we generate 50 queries at each iteration for sparse recovery and determine if attack successes before 200 iterations. At each iteration of sparse recovery, we randomly select a subspace of 2000 dimensions (pixels) and generate random perturbations only in this subspace. We note that sparse adversarial attacks have been investigated before; see, for example, SparseFool (Modas et al., 2019). To the best of our knowledge, we are the first to connect adversarial attacks to sparse coding based zeroth-order optimization.

We present the detailed experimental results in Table 1. Note that the attack success rate of ZORO is best among all methods, while its average distortion ℓ_0 loss is smaller than ZO-SCD. Surprisingly, the average distortion ℓ_2 loss of ZORO attacks is also the best among all zeroth-order methods. Note that the average iterations of ZORO is the best among all methods, but the average query is the worst since it uses more queries at each iteration.

We further consider applying a median filter in order to mitigate the adversarial attack. We use Inception-V3 on the attacked-then-filtered image to check if the model identifies the true label, that is, if the attack has been mitigated. We also apply the same filter to the original image to check if the median filter reduces model accuracy on un-attacked images. We summarize the total reduction in prediction accuracy on the set of adversarial and original images due to the mitigated adversarial attacks and the distortion from median filter. The results are shown in Table 2. We note that with a median filter, there is a good chance that the attacks can be mitigated. The catch is that the median filter also distorts the original images and reduces the models classification accuracy.

Table 1: Attack success rate (ASR), average final ℓ_0 distortion (as a percentage of the total number of pixels), average final ℓ_2 distortion, and average iterations of first successful attack for different zeroth-order attack methods.

METHODS	ASR	ℓ_0 DIST	ℓ_2 DIST	ITER
ZO-SCD	78 %	0.89%	57.5	240
ZO-SGD	78%	100%	37.9	159
ZO-AdaMM	81%	100%	28.2	172
ZORO	90%	0.73%	21.1	59

Table 2: Recovery success rate (RSR), original image distortion rate, and total prediction accuracy reduction for different median filter sizes.

MEDIAN FILTER	RSR	DIST RATE	TOT REDUCTION
size = 2	86 %	8%	21%
size = 3	92 %	7%	14%
size = 4	76 %	14%	34%
size = 5	69 %	29%	53%

Acknowledgments

The work of the first two authors was partially supported by NSF Grant DMS-1720237 and ONR Grant N000141712162. The authors would like to thank Drs. Rong Jin and Jian Tan for helpful discussions.

References

Agarwal, A., Dekel, O., and Xiao, L. Optimal algorithms for online convex optimization with multi-point bandit feedback. In *COLT*, pp. 28–40. Citeseer, 2010.

Balasubramanian, K. and Ghadimi, S. Zeroth-order (non)-convex stochastic optimization via conditional gradient and gradient updates. In *Advances in Neural Information Processing Systems*, pp. 3455–3464, 2018.

Baraniuk, R., Davenport, M., DeVore, R., and Wakin, M. A simple proof of the restricted isometry property for random matrices. *Constructive Approximation*, 28(3):253–263, 2008.

Chang, T.-J., Meade, N., Beasley, J. E., and Sharaiha, Y. M. Heuristics for cardinality constrained portfolio optimisation. *Computers & Operations Research*, 27(13):1271–1302, 2000.

Chen, X., Liu, S., Xu, K., Li, X., Lin, X., Hong, M., and Cox, D. Zo-adamm: Zeroth-order adaptive momentum method for black-box optimization. In *Advances in Neural Information Processing Systems*, pp. 7202–7213, 2019.

Choromanski, K., Rowland, M., Sindhwani, V., Turner, R. E., and Weller, A. Structured evolution with compact architectures for scalable policy optimization. *arXiv preprint arXiv:1804.02395*, 2018.

Deng, J., Dong, W., Socher, R., Li, L.-J., Li, K., and Fei-Fei, L. Imagenet: A large-scale hierarchical image database. In *2009 IEEE conference on computer vision and pattern recognition*, pp. 248–255. Ieee, 2009.

Duchi, J. C., Jordan, M. I., Wainwright, M. J., and Wibisono, A. Optimal rates for zero-order convex optimization: The power of two function evaluations. *IEEE Transactions on Information Theory*, 61(5):2788–2806, 2015.

Fan, J. and Li, R. Variable selection via nonconcave penalized likelihood and its oracle properties. *Journal of the American statistical Association*, 96(456):1348–1360, 2001.

Flaxman, A. D., Kalai, A. T., and McMahan, H. B. Online convex optimization in the bandit setting: gradient descent without a gradient. *arXiv preprint cs/0408007*, 2004.

Foucart, S. Sparse recovery algorithms: sufficient conditions in terms of restricted isometry constants. In *Approximation Theory XIII: San Antonio 2010*, pp. 65–77. Springer, 2012.

Friedlander, M. P. and Schmidt, M. Hybrid deterministic-stochastic methods for data fitting. *SIAM Journal on Scientific Computing*, 34(3):A1380–A1405, 2012.

Ghadimi, S. and Lan, G. Stochastic first-and zeroth-order methods for nonconvex stochastic programming. *SIAM Journal on Optimization*, 23(4):2341–2368, 2013.

Gu, B., Huo, Z., Deng, C., and Huang, H. Faster derivative-free stochastic algorithm for shared memory machines. In *International Conference on Machine Learning*, pp. 1812–1821, 2018.

Jamieson, K. G., Nowak, R., and Recht, B. Query complexity of derivative-free optimization. In *Advances in Neural Information Processing Systems*, pp. 2672–2680, 2012.

Kiefer, J., Wolfowitz, J., et al. Stochastic estimation of the maximum of a regression function. *The Annals of Mathematical Statistics*, 23(3):462–466, 1952.

Kurakin, A., Goodfellow, I., and Bengio, S. Adversarial machine learning at scale. *arXiv preprint arXiv:1611.01236*, 2016.

Larson, J., Menickelly, M., and Wild, S. M. Derivative-free optimization methods. *Acta Numerica*, 28:287–404, 2019.

Lian, X., Zhang, H., Hsieh, C.-J., Huang, Y., and Liu, J. A comprehensive linear speedup analysis for asynchronous stochastic parallel optimization from zeroth-order to first-order. In *Advances in Neural Information Processing Systems*, pp. 3054–3062, 2016.

Liu, S., Chen, J., Chen, P.-Y., and Hero, A. Zeroth-order online alternating direction method of multipliers: Convergence analysis and applications. In *International Conference on Artificial Intelligence and Statistics*, pp. 288–297, 2018.

Liu, S., Chen, P. Y., Chen, X., and Hong, M. Signs gd via zeroth-order oracle. In *7th International Conference on Learning Representations, ICLR 2019*, 2019.

Modas, A., Moosavi-Dezfooli, S.-M., and Frossard, P. Sparsefool: a few pixels make a big difference. In *Proceedings of the IEEE Conference on Computer Vision and Pattern Recognition*, pp. 9087–9096, 2019.

Nakamura, N., Seepaul, J., Kadane, J. B., and Reeja-Jayan, B. Design for low-temperature microwave-assisted crystallization of ceramic thin films. *Applied Stochastic Models in Business and Industry*, 33(3):314–321, 2017.

Needell, D. and Tropp, J. A. Cosamp: Iterative signal recovery from incomplete and inaccurate samples. *Applied and computational harmonic analysis*, 26(3):301–321, 2009.

Nesterov, Y. and Spokoiny, V. Random gradient-free minimization of convex functions. *Technical report, Universite catholique de Louvain, Center for Operations Research and Econometrics (CORE)*, 2011.

Nesterov, Y. and Spokoiny, V. Random gradient-free minimization of convex functions. *Foundations of Computational Mathematics*, 17(2):527–566, 2017.

Papernot, N., McDaniel, P., Goodfellow, I., Jha, S., Celik, Z. B., and Swami, A. Practical black-box attacks against machine learning. In *Proceedings of the 2017 ACM on Asia conference on computer and communications security*, pp. 506–519, 2017.

Schmidt, M., Roux, N. L., and Bach, F. R. Convergence rates of inexact proximal-gradient methods for convex optimization. In *Advances in neural information processing systems*, pp. 1458–1466, 2011.

Schöpfer, F. Linear convergence of descent methods for the unconstrained minimization of restricted strongly convex functions. *SIAM Journal on Optimization*, 26(3):1883–1911, 2016.

Shamir, O. On the complexity of bandit and derivative-free stochastic convex optimization. In *Conference on Learning Theory*, pp. 3–24, 2013.

Snoek, J., Larochelle, H., and Adams, R. P. Practical bayesian optimization of machine learning algorithms. In *Advances in neural information processing systems*, pp. 2951–2959, 2012.

Spall, J. C. An overview of the simultaneous perturbation method for efficient optimization. *Johns Hopkins apl technical digest*, 19(4):482–492, 1998.

Szegedy, C., Vanhoucke, V., Ioffe, S., Shlens, J., and Wojna, Z. Rethinking the inception architecture for computer vision. In *Proceedings of the IEEE conference on computer vision and pattern recognition*, pp. 2818–2826, 2016.

Taskar, B., Chatalbashev, V., Koller, D., and Guestrin, C. Learning structured prediction models: A large margin approach. In *Proceedings of the 22nd international conference on Machine learning*, pp. 896–903, 2005.

Tikhomirov, K. Singularity of random bernoulli matrices. *Annals of Mathematics*, 191(2):593–634, 2020.

Wang, Y., Du, S., Balakrishnan, S., and Singh, A. Stochastic zeroth-order optimization in high dimensions. In *International Conference on Artificial Intelligence and Statistics*, pp. 1356–1365, 2018.

Wang, Z., Zoghi, M., Hutter, F., Matheson, D., and De Freitas, N. Bayesian optimization in high dimensions via random embeddings. In *Twenty-Third International Joint Conference on Artificial Intelligence*, 2013.

Zhang, H. The restricted strong convexity revisited: analysis of equivalence to error bound and quadratic growth. *Optimization Letters*, 11(4):817–833, 2017.

Zhang, H. and Cheng, L. Restricted strong convexity and its applications to convergence analysis of gradient-type methods in convex optimization. *Optimization Letters*, 9(5):961–979, 2015.

ZORO: Supplemental Materials

In this supplementary material we provide the proofs for the main theorems presented in the main article and present the results of some additional numerical experiments. Specifically, in Section A we present the proofs for Section 3 in the main article, which center around the accuracy of the gradient estimator used in ZORO. Section B contains several technical results on sequences and inexact gradient descent, and culminates in the proofs of Theorems 4.1 and 4.2. In Section C we present the proofs of our main results, namely those contained in section 5, while in Section D we present some additional numerical results that may be of interest.

Before proceeding, for the reader's convenience, we provide a table of notation here (see Table 3).

Table 3: Table of Notation.

NOTATION	DEFINITION
d	dimension of x
$f(x)$	underlying loss function
s	sparsity of ∇f (when it is sparse)
$r(x)$	regularization function
$F(x)$	$f(x) + r(x)$, if r is non-zero
$\min F$	$\min\{F(x) : x \in \mathbb{R}^d\}$, minimum value of F
e_k	$F(x_k) - \min F$, objective error
x_k	k -th iterate of ZORO
z_i	Rademacher random variable, see (10)
n	number of iterations of CoSaMP in ZORO
\mathbf{g}_k	$\nabla f(x_k)$, true gradient at x_k
$\hat{\mathbf{g}}_k$	estimated gradient at x_k
\mathbf{e}_k	$\hat{\mathbf{g}}_k - \mathbf{g}_k$, gradient estimation error
$\tilde{\nabla}r$	∂r picked out by the proximal operator
$\hat{\Delta}_k$	$-(\tilde{\nabla}r(x_{k+1}) + \hat{\mathbf{g}}_k)$
Δ_k	$-(\tilde{\nabla}r(x_{k+1}) + \mathbf{g}_k)$
$\tilde{\Delta}_k$	$-(\tilde{\nabla}r(x_{k+1}) + \mathbf{g}_{k+1})$
H	uniform bound of $\ \nabla^2 f\ _1$ (Asm. 2)
L	Lipschitz constant of ∇f (Asm. 3)
ν	restricted strong convexity of f (Def. 2)
$E_f(x)$	oracle query of $f(x)$, see (2)
ξ	oracle noise
σ	bound of ξ (Asm. 4)
m	number of samples
δ	sampling radius, see (11)
$\ \cdot\ _0$	ℓ_0 -norm
$\ \cdot\ _1$	ℓ_1 -norm
$\ \cdot\ _2$	ℓ_2 -norm
$\ \cdot\ _\infty$	ℓ_∞ -norm
$[\cdot]_{(s)}$	best s -sparse approximate
$P_*(\cdot)$	projection onto the solution set
$\mathbb{P}[\cdot]$	probability
$\mathbb{E}[\cdot]$	expectation

A Proofs for Section 3

Proof of Lemma 3.1. The proof is similar to the argument of Section 3 in (Wang et al., 2018), but we include it for completeness. From Taylor's theorem:

$$f(x + \delta z_i) = f(x) + \delta z_i^\top \mathbf{g} + \frac{\delta^2}{2} z_i^\top \nabla^2 f(x + tz_i) z_i$$

for some $t \in (0, 1)$. Assuming $E_f(x + \delta z_i) = f(x + \delta z_i) + \xi_+$ and $E_f(x) = f(x) + \xi_-$, equation (11) becomes:

$$\begin{aligned} y_i &= \frac{1}{\sqrt{m}} z_i^\top \mathbf{g} + \frac{\xi_+ - \xi_-}{\sqrt{m}} \\ &\quad + \frac{\delta}{2\sqrt{m}} z_i^\top \nabla^2 f(x + tz_i) z_i. \end{aligned}$$

Let $\mu_i := \frac{\xi_+ - \xi_-}{\sqrt{m}}$, then $|\mu_i| \leq 2\sigma/\sqrt{m}$. Let $\nu_i = z_i^\top \nabla^2 f(x + tz_i) z_i/(2\sqrt{m})$. Now:

$$\begin{aligned} 2\sqrt{m}|\nu_i| &= |z_i^\top \nabla^2 f(x + t_0 \delta z_i) z_i| \\ &= \left| \sum_{j,k} \nabla_{j,k}^2 f(x + t_0 \delta z_i) (z_i)_j (z_i)_k \right| \\ &\leq \|\nabla^2 f(x + t_0 \delta z_i)\|_1 \|z_i\|_\infty^2 \leq H \end{aligned}$$

by Assumption 2 and the fact that $\|z_i\|_\infty = 1$. \square

For future use, let $\boldsymbol{\mu} = [\mu_1, \dots, \mu_m]^\top$ and $\boldsymbol{\nu} = [\nu_1, \dots, \nu_m]^\top$. Then:

$$\mathbf{y} = Z\mathbf{g} + \frac{1}{\delta} \boldsymbol{\mu} + \delta \boldsymbol{\nu}. \quad (18)$$

A.1 Proof of Theorem 3.2

For the convenience of the reader we begin by recalling a few theorems from the literature.

Theorem A.1 (Theorem 5.2 of (Baraniuk et al., 2008)). *If $m = b_1 s \log(d/s)$ then Z satisfies the Restricted Isometry Property (RIP) with constant $\delta_{4s}(Z) \leq 0.3843$ with probability $1 - (s/d)^{b_2 s}$. Here b_1 and b_2 are constants independent of s, d and m .*

We remind the reader that Z has the $(4s)$ -RIP if, for all $\mathbf{v} \in \mathbb{R}^d$ with $\|\mathbf{v}\|_0 \leq 4s$:

$$(1 - \delta_{4s}(Z))\|\mathbf{v}\|_2^2 \leq \|Z\mathbf{v}\|_2^2 \leq (1 + \delta_{4s}(Z))\|\mathbf{v}\|_2^2.$$

The choice of the value 0.3843 is to match with the assumptions of (Foucart, 2012), which we state next. Recall that $[\mathbf{g}]_{(s)}$ denotes the best s -sparse approximation to \mathbf{g} .

Theorem A.2 (Theorem 5 of (Foucart, 2012)). *Let $\{\mathbf{g}^n\}$ be the sequence generated by applying CoSaMP (Needell & Tropp, 2009) to problem (12), with $m \geq b_1 s \log(d/s)$ and initialization $\mathbf{g}^0 = \mathbf{0}$. Then, with probability $1 - (s/d)^{b_2 s}$: for all \mathbf{g} ,*

$$\|\mathbf{g}^n - [\mathbf{g}]_{(s)}\|_2 \leq \tau \left\| Z(\mathbf{g} - [\mathbf{g}]_{(s)}) + \frac{1}{\delta} \boldsymbol{\mu} + \delta \boldsymbol{\nu} \right\|_2 + \rho^n \left\| [\mathbf{g}]_{(s)} \right\|_2, \quad (19)$$

where $\rho < 1$ and $\tau \approx 10$ depend only on δ_{4s} .

The exact values of ρ and τ are provided in (Foucart, 2012). Note that the constants b_1, b_2 are the same as in Theorem A.1. Certainly, other initializations are possible. For example, when using the ZORO method we have found that taking \mathbf{g}^0 to be the gradient estimator found at the previous step, *i.e.* $\mathbf{g}^0 = \hat{\mathbf{g}}_{k-1}$, offers a modest speed-up.

Theorem A.3 (Proposition 3.5 in (Needell & Tropp, 2009)). *Suppose that Z satisfies the $(4s)$ -RIP. Then for any $\mathbf{v} \in \mathbb{R}^d$:*

$$\|Z\mathbf{v}\|_2 \leq \sqrt{1 + \delta_{4s}(Z)} \left(\|\mathbf{v}\|_2 + \frac{1}{\sqrt{s}} \|\mathbf{v}\|_1 \right).$$

Theorem A.4 (Concentration of measure). *Suppose that $Z = \frac{1}{\sqrt{m}}A \in \mathbb{R}^{m \times d}$ where:*

$$A_{ij} = \begin{cases} +1 & \text{with probability } 1/2, \\ -1 & \text{with probability } 1/2. \end{cases}$$

Then for any $\varepsilon > 0$ and any $\mathbf{v} \in \mathbb{R}^d$:

$$\mathbb{P} [|\|Z\mathbf{v}\|_2^2 - \|\mathbf{v}\|_2^2| \geq \varepsilon \|\mathbf{v}\|_2^2] \leq 2e^{-mb_3(\varepsilon)}$$

where $b_3(\varepsilon) := \varepsilon^2/4 - \varepsilon^3/6$.

Proof. See, for example, Section 4 of (Baraniuk et al., 2008) and references contained therein. \square

Note that it follows from (19) that:

$$\|\mathbf{g}^n - \mathbf{g}\|_2 \leq \|\mathbf{g} - [\mathbf{g}]_{(s)}\|_2 + \tau \|Z(\mathbf{g} - [\mathbf{g}]_{(s)})\|_2 + \frac{\tau}{\delta} \|\boldsymbol{\mu}\|_2 + \tau \delta \|\boldsymbol{\nu}\|_2 + \rho^n \|[\mathbf{g}]_{(s)}\|_2. \quad (20)$$

Lemma A.5. *Suppose f satisfies Assumption 1.b. Then $\|\mathbf{g} - [\mathbf{g}]_{(s)}\|_2 + \tau \|Z(\mathbf{g} - [\mathbf{g}]_{(s)})\|_2 \leq \psi \|\mathbf{g}\|_2$ where:*

$$\psi = \left(\left(1 + \tau \sqrt{1 + \delta_{4s}(Z)} \right) \left(\frac{2}{p} - 1 \right)^{-1/2} + \tau \sqrt{1 + \delta_{4s}(Z)} \left(\frac{1}{p} - 1 \right)^{-1} \right) s^{1/2-1/p}.$$

Proof. Combining the bounds (4),(5) and Theorem A.3 we obtain:

$$\begin{aligned} \|Z(\mathbf{g} - [\mathbf{g}]_{(s)})\|_2 &\leq \sqrt{1 + \delta_{4s}(Z)} \left(\|\mathbf{g} - [\mathbf{g}]_{(s)}\|_2 + \frac{1}{\sqrt{s}} \|\mathbf{g} - [\mathbf{g}]_{(s)}\|_1 \right) \\ &\leq \sqrt{1 + \delta_{4s}(Z)} \left(\left(\frac{2}{p} - 1 \right)^{-1/2} \|\mathbf{g}\|_2 s^{1/2-1/p} + \frac{1}{\sqrt{s}} \left(\frac{1}{p} - 1 \right)^{-1} \|\mathbf{g}\|_2 s^{1-1/p} \right) \\ &= \sqrt{1 + \delta_{4s}(Z)} \left(\left(\frac{2}{p} - 1 \right)^{-1/2} + \left(\frac{1}{p} - 1 \right)^{-1} \right) s^{1/2-1/p} \|\mathbf{g}\|_2. \end{aligned}$$

Use (5) again to bound $\|\mathbf{g} - [\mathbf{g}]_{(s)}\|_2$ and add to obtain the lemma. \square

Lemma A.6. $\|\boldsymbol{\mu}\|_2 \leq 2\sigma$ and $\|\boldsymbol{\nu}\|_2 \leq H/2$.

Proof. From Lemma 3.1, we have

$$\|\boldsymbol{\mu}\|_2^2 = \sum_{i=1}^m \mu_i^2 \leq \sum_{i=1}^m \frac{4\sigma^2}{m} = 4\sigma^2.$$

Similarly, we also get

$$\|\boldsymbol{\nu}\|_2^2 = \sum_{i=1}^m \nu_i^2 \leq \sum_{i=1}^m \frac{H^2}{4m} = \frac{H^2}{4}.$$

□

Combining Lemmas A.5 and A.6 with (20), and using $\|[\mathbf{g}]_{(s)}\|_2 \leq \|\mathbf{g}\|_2$, yields Theorem 3.2.

B Proofs for Section 4

B.1 Proofs for Theorem 4.1 and 4.2

We proceed via a series of Lemmas.

Lemma B.1 (Sequence analysis). *Consider a sequence $e_k \geq 0$ obeying $e_{k+1} \leq e_k - ce_k^2 + d$ for $k = 0, 1, \dots$ where $c > 0$ and $d \geq 0$. We have*

$$e_k \leq \frac{e_0}{e_0 c \cdot k + 2}, \quad k \in \{t : e_0, \dots, e_{t+1} \geq \sqrt{2d/c}\}.$$

In particular, if $d = 0$, then we get

$$e_k \leq \frac{e_0}{e_0 c \cdot k + 1}, \quad k = 0, 1, \dots$$

The first result is a decay of e_k at rate $\sim 1/(ck)$ up until $e_k = \sqrt{2d/c}$. The second result has the rate $\sim 1/(ck)$ for all k .

Proof. Without loss of generality, assume $e_k > 0$ for $k = 0, 1, \dots$. If $e_k \geq \sqrt{2d/c}$, then $e_{k+1} \leq e_k - d$, so $\frac{e_k}{e_{k+1}} \geq 1$. Dividing the condition by $e_{k+1}e_k$ and reorganizing yields

$$\begin{aligned} \frac{1}{e_{k+1}} - \frac{1}{e_k} &\geq \frac{ce_k}{e_{k+1}} - \frac{d}{e_{k+1}e_k} \\ &\geq \begin{cases} c - \frac{d}{2d/c} = \frac{1}{2}c, & d \neq 0, \\ c, & d = 0. \end{cases} \end{aligned}$$

Summing, we obtain $\frac{1}{e_k} \geq \frac{1}{e_0} + \frac{1}{2}kc$ when $d \neq 0$ and $\frac{1}{e_k} \geq \frac{1}{e_0} + kc$ when $d = 0$. Inverting both sides yields the claim. Note that we have assumed that $e_{k+1} \geq \sqrt{2d/c}$ in the $d \neq 0$ case. □

Lemma B.2 (Sequence analysis). *Any nonnegative sequence e_k obeying $ae_k \leq b(e_k - e_{k+1}) + c_k$ for $b > a > 0$ and $c_k \geq 0$ satisfies*

$$e_k \leq \frac{(b-a)^k e_0}{b^k} + \sum_{t=1}^k \frac{(b-a)^{t-1} c_{k-t}}{b^t}.$$

On the right-hand side, the first term presents geometric convergence at rate $(b-a)/b$ and the second term is accumulated noise.

Proof. The condition gives us $be_{k+1} \leq (b-a)e_k + c_k$ and thus $e_{k+1} \leq \frac{b-a}{b}e_k + \frac{c_k}{b}$. Repeatedly applying this inequality produces the result. \square

The next lemma quantifies, under very general assumptions, the amount of descent per iteration of prox-gradient descent we can expect with an inexact gradient estimate.

Lemma B.3. *Suppose that $f(x)$ satisfies Assumption 3 and that $\alpha < 2/L$ if $r(x)$ is convex, while $\alpha < 1/L$ if $r(x)$ is non-convex. Then if $x_{k+1} = x_k - \alpha \hat{g}_k$:*

$$F(x_{k+1}) \leq F(x_k) - \frac{c_0}{2} \|\alpha \hat{\Delta}_k\|_2^2 + \frac{1}{2c_0} \|\mathbf{g}_k - \hat{\mathbf{g}}_k\|_2^2 \quad (21)$$

$$F(x_{k+1}) \leq F(x_k) - c_1 \|\alpha \Delta_k\|_2^2 + c_2 \|\mathbf{g}_k - \hat{\mathbf{g}}_k\|_2^2 \quad (22)$$

$$F(x_{k+1}) \leq F(x_k) - c_3 \|\alpha \tilde{\Delta}_k\|_2^2 + c_4 \|\mathbf{g}_k - \hat{\mathbf{g}}_k\|_2^2 \quad (23)$$

where $c_0 = \frac{2-1_{\text{ncvx}}-\alpha L}{2\alpha}$, $c_1^{\text{ncvx}=1} = \frac{1-\alpha L}{4\alpha}$, $c_1^{\text{ncvx}=0} = \frac{(1-\alpha L)^2+1}{2\alpha^2 L}$, $c_2^{\text{ncvx}=1} = \frac{\alpha^3 L^2+\alpha}{2-2\alpha L}$, $c_2^{\text{ncvx}=0} = \frac{\alpha^2 L}{4}$, $c_3 = (\frac{2}{c_1} + \frac{4\alpha^2 L^2}{c_0})^{-1}$ and $c_4 = c_3(\frac{2c_2}{c_1} + \frac{2\alpha^2 L^2}{c_0^2})$.

Proof. We begin by expanding F .

$$F(x_{k+1}) - F(x_k) = f(x_{k+1}) - f(x_k) + r(x_{k+1}) - r(x_k). \quad (24)$$

When r is convex, we get from the first-order optimality condition of $\text{prox}_{\alpha r}$: $\tilde{\nabla}r(x_{k+1}) = -\hat{\Delta}_k - \alpha \hat{g}_k$ and, by convexity of r ,

$$r(x_{k+1}) - r(x_k) \leq \langle \tilde{\nabla}r(x_{k+1}), \alpha \hat{\Delta}_k \rangle = -\langle \alpha \hat{\Delta}_k, \hat{g}_k \rangle - \alpha \|\hat{\Delta}_k\|_2^2.$$

When r is nonconvex, by expanding the definition of $\text{prox}_{\alpha r}$ and comparing the optimal $x = x_{k+1}$ to non-optimal $x = x_k$, we can get

$$r(x_{k+1}) - r(x_k) \leq -\langle \alpha \hat{\Delta}_k, \hat{g}_k \rangle - \frac{\alpha}{2} \|\hat{\Delta}_k\|_2^2.$$

Note that $\frac{\alpha}{2} < \alpha$ means the last inequality is weaker than the one above it.

Now for $f(x_{k+1}) - f(x_k)$ in (24), apply smoothness of $f(x)$ (Assumption 3) to get:

$$\begin{aligned} f(x_{k+1}) - f(x_k) &\leq \langle \alpha \hat{\Delta}_k, \mathbf{g}_k \rangle + \frac{L}{2} \|\alpha \hat{\Delta}_k\|_2^2 \\ &= \langle \alpha \hat{\Delta}_k, \hat{g}_k \rangle + \frac{L}{2} \|\alpha \hat{\Delta}_k\|_2^2 + \langle \alpha \hat{\Delta}_k, \mathbf{g}_k - \hat{g}_k \rangle. \end{aligned}$$

Adding the bounds for $r(x_{k+1}) - r(x_k)$ and $f(x_{k+1}) - f(x_k)$ yields:

$$\begin{aligned} F(x_{k+1}) - F(x_k) &\leq -\underbrace{\left(\frac{1}{(1+1_{\text{ncvx}})\alpha} - \frac{L}{2} \right)}_{c_0} \|\alpha \hat{\Delta}_k\|_2^2 + \langle \alpha \hat{\Delta}_k, \mathbf{g}_k - \hat{g}_k \rangle \\ &\stackrel{(a)}{\leq} -c_0 \|\alpha \hat{\Delta}\|_2^2 + \frac{c_0}{2} \|\alpha \hat{\Delta}\|_2^2 + \frac{1}{2c_0} \|\mathbf{g}_k - \hat{g}_k\|_2^2 = -\frac{c_0}{2} \|\alpha \hat{\Delta}\|_2^2 + \frac{1}{2c_0} \|\mathbf{g}_k - \hat{g}_k\|_2^2 \end{aligned} \quad (25)$$

Where we have used Young's inequality to obtain (a). For the second inequality, we return to (25) and apply $\hat{\Delta}_k = \Delta_k + (\mathbf{g}_k - \hat{\mathbf{g}}_k)$. This yields:

$$\begin{aligned} F(x_{k+1}) - F(x_k) &\leq -c_0 \|\alpha \Delta_k\|_2^2 + (1 - 2\alpha c_0) \langle \alpha \Delta_k, \mathbf{g}_k - \hat{\mathbf{g}}_k \rangle + (\alpha - \alpha^2 c_0) \|\mathbf{g}_k - \hat{\mathbf{g}}_k\|_2^2 \\ &\stackrel{(a)}{\leq} - \underbrace{\left(c_0 - \frac{(1 - 2\alpha c_0)q}{2} \right)}_{c_1} \|\alpha \Delta_k\|_2^2 + \underbrace{\left(\frac{1 - 2\alpha c_0}{2q} + \alpha - \alpha^2 c_0 \right)}_{c_2} \|\mathbf{g}_k - \hat{\mathbf{g}}_k\|_2^2 \end{aligned}$$

where (a) follows again from Young's inequality, for any $q > 0$. As c_1 and c_2 must be positive, we require $0 < q < \frac{1-\alpha L}{\alpha^2 L}$ when $1_{\text{ncvx}} = 1$ and $q > \frac{1-\alpha L}{\alpha^2 L}$ when $1_{\text{ncvx}} = 0$. In particular, we pick $q = \frac{1-\alpha L}{2\alpha^2 L}$ when $1_{\text{ncvx}} = 1$ and $q = \frac{2-2\alpha L}{\alpha^2 L}$ when $1_{\text{ncvx}} = 0$ for this proof.

Finally, observe that:

$$\begin{aligned} \|\tilde{\Delta}_k\|_2 &\stackrel{(a)}{=} \| -\tilde{\nabla}r(x_{k+1}) - \mathbf{g}_{k+1} \|_2 = \| -\tilde{\nabla}r(x_{k+1}) - \mathbf{g}_k + \mathbf{g}_k - \mathbf{g}_{k+1} \|_2 \\ &\stackrel{(b)}{\leq} \|\Delta_k\|_2 + \|\mathbf{g}_k - \mathbf{g}_{k+1}\|_2 \stackrel{(c)}{\leq} \|\Delta_k\|_2 + \alpha L \|\hat{\Delta}_k\|_2 \end{aligned}$$

Where (a) follows from the definition of $\tilde{\Delta}_k$, (b) follows from the definition of Δ_k and (c) follows from smoothness of $f(x)$ (Assumption 3). Thus, we have that $\|\tilde{\Delta}_k\|_2^2 \leq 2\|\Delta_k\|_2^2 + 2\alpha^2 L^2 \|\hat{\Delta}_k\|_2^2$. Therefore, combining (21) and (22) yields (23). In particular, $c_3 = (\frac{2}{c_1} + \frac{4\alpha^2 L^2}{c_0})^{-1}$ and $c_4 = c_3(\frac{2c_2}{c_1} + \frac{2\alpha^2 L^2}{c_0^2})$. \square

Note that an immediate consequence of this lemma is the following:

Lemma B.4. *Suppose that $f(x)$ satisfies Assumption 3, that $r(x)$ is proximable and that $\alpha < 2/L$ if $r(x)$ is convex while $\alpha < 1/L$ if $r(x)$ is non-convex. Then:*

$$\begin{aligned} \sum_{t=0}^k \|\alpha \hat{\Delta}_t\|_2^2 &\leq \hat{c}_5 (F(x_0) - F(x_*)) + \hat{c}_6 \sum_{t=0}^k \|\hat{\mathbf{g}}_t - \mathbf{g}_t\|_2^2 \\ \sum_{t=0}^k \|\alpha \Delta_t\|_2^2 &\leq c_5 (F(x_0) - F(x_*)) + c_6 \sum_{t=0}^k \|\hat{\mathbf{g}}_t - \mathbf{g}_t\|_2^2 \\ \sum_{t=0}^k \|\alpha \tilde{\Delta}_t\|_2^2 &\leq \tilde{c}_5 (F(x_0) - F(x_*)) + \tilde{c}_6 \sum_{t=0}^k \|\hat{\mathbf{g}}_t - \mathbf{g}_t\|_2^2 \end{aligned}$$

for constants $\hat{c}_5 = \frac{2}{c_0}$, $\hat{c}_6 = \frac{1}{c_0^2}$, $c_5 = \frac{1}{c_1}$, $c_6 = \frac{c_2}{c_1}$, $\tilde{c}_5 = \frac{1}{c_3}$ and $\tilde{c}_6 = \frac{c_4}{c_3}$.

Proof. Take the telescopic sums of (21), (22) and (23) respectively. Then, use the fact that by Assumption 3 a minimizer of $F(x)$, namely x_* , exists. Hence $F(x_0) - F(x_k) \leq F(x_0) - F(x_*)$ \square

The next lemma prepares the conditions for us to apply Lemma B.1. Recall that $P_*(\cdot)$ is a projection operator onto the solution set.

Lemma B.5. *Suppose that $F(x)$ is convex and that $f(x)$ satisfies Assumption 3. Then:*

$$e_k^2 \leq c_7 \|x_k - P_*(x_k)\|_2^2 (e_k - e_{k+1}) + c_8 \|x_k - P_*(x_k)\|_2^2 \|\mathbf{g}_k - \hat{\mathbf{g}}_k\|_2^2 \quad (26)$$

for $c_7 = \frac{1}{\alpha^2 c_3}$ and $c_8 = \frac{c_4}{\alpha^2 c_3}$. If, in addition, $r(x) = 0$ and $\|\mathbf{g}_k - \hat{\mathbf{g}}_k\|_2 \leq \varepsilon_{\text{rel}} \|\mathbf{g}_k\|_2$, then

$$e_k^2 \leq c_9 \|x_k - P_*(x_k)\|_2^2 (e_k - e_{k+1}) \quad (27)$$

for $c_9 = \frac{4}{\alpha(2(1-\varepsilon_{\text{rel}}^2)-\alpha L(1+\varepsilon_{\text{rel}}^2))}$.

Proof. By existence of $P_*(x_k)$ and convexity of $F(x)$,

$$\begin{aligned} e_k &= F(x_k) - F(P_*(x_k)) \leq \langle \tilde{\Delta}_k, x_k - P_*(x_k) \rangle \\ &\leq \|\tilde{\Delta}_k\|_2 \|x_k - P_*(x_k)\|_2 \\ \Rightarrow e_k^2 &\leq \|\tilde{\Delta}_k\|_2^2 \|x_k - P_*(x_k)\|_2^2 \end{aligned} \quad (28)$$

It remains to bound $\|\tilde{\Delta}_k\|_2^2$. By (23), we get

$$c_3 \alpha^2 \|\tilde{\Delta}_k\|_2^2 \leq e_k - e_{k+1} + c_4 \|\mathbf{g}_k - \hat{\mathbf{g}}_k\|_2^2.$$

Substituting this into (28) yields the first claim.

Now suppose that, in addition, $r(x) = 0$ and $\|\mathbf{g}_k - \hat{\mathbf{g}}_k\|_2 \leq \varepsilon_{\text{rel}} \|\mathbf{g}_k\|_2$. In this case:

$$\begin{aligned} e_k &= f(x_k) - f(P_*(x_k)) \leq \langle \mathbf{g}_k, x_k - P_*(x_k) \rangle \\ &\leq \|\mathbf{g}_k\|_2 \|x_k - P_*(x_k)\|_2 \\ \Rightarrow e_k^2 &\leq \|x_k - P_*(x_k)\|_2^2 \|\mathbf{g}_k\|_2^2. \end{aligned} \quad (29)$$

Using smoothness of $f(x)$, Young's inequality and the bound $\|\mathbf{g}_k - \hat{\mathbf{g}}_k\|_2 \leq \varepsilon_{\text{rel}} \|\mathbf{g}_k\|_2$ we may obtain:

$$\frac{1}{2} (\alpha^2 c_0 - \alpha^2 \varepsilon_{\text{rel}}^2 (c_0 + L)) \|\mathbf{g}_k\|_2^2 \leq e_k - e_{k+1},$$

where $c_0 = \frac{1}{\alpha} - \frac{L}{2}$. (This is equivalent to (22) when $r(x) = 0$). Substituting this into (29) yields the second claim. \square

Proof of Theorem 4.1. Rearranging (26) to fit the hypothesis of Lemma B.1 we get:

$$e_{k+1} \leq e_k - \frac{1}{c_7 R^2} e_k^2 + \frac{c_8}{c_7} \varepsilon_{\text{abs}}$$

where we are using the assumption $\|x_k - P_*(x_k)\|_2 \leq R$ as well as the fact that $\|\mathbf{g}_k - \hat{\mathbf{g}}_k\|_2 \leq \varepsilon_{\text{abs}}$. Applying Lemma B.1 yields the Part 1.

Rearranging (27) to fit the hypothesis of Lemma B.1, with $d = 0$, we get:

$$e_k^2 \leq c_9 R^2 (e_k - e_{k+1})$$

where again we have used $\|x_k - P_*(x_k)\|_2 \leq R$. Applying Lemma B.1 again proves Part 2. \square

Proof of Theorem 4.2. Substituting (8) into the results of Lemma B.5 and dividing by a factor of e_k results in

$$\nu e_k \leq c_7 (e_k - e_{k+1}) + c_8 \|\mathbf{g}_k - \hat{\mathbf{g}}_k\|_2^2,$$

and if $\|\mathbf{g}_k - \hat{\mathbf{g}}_k\|_2 \leq \varepsilon_{\text{rel}} \|\mathbf{g}_k\|_2$,

$$\nu e_k \leq c_9(e_k - e_{k+1}).$$

The claims then directly follow from Lemma B.2. In particular, when $\|\mathbf{g}_k - \hat{\mathbf{g}}_k\|_2^2 \leq \varepsilon_{\text{abs}}$ for all k , we have $\sum_{t=1}^{\infty} c_{10}^{t-1} c_{11} \|\mathbf{g}_k - \hat{\mathbf{g}}_k\|_2^2 \leq (1 - c_{10})^{-1} c_{11} \varepsilon_{\text{abs}}$. \square

Proof of Theorem 4.3. Follows directly from Lemma B.4. \square

B.2 Boundedness results

In this section, we establish various conditions under which the sequence of iterates, x_k , is bounded. For notational convenience, define $\mathbf{e}_k := \hat{\mathbf{g}}_k - \mathbf{g}_k$.

Proposition B.6. *Assume f is convex. Then there exists an R such that $\|x_k - \mathbf{P}_*(x_k)\|_2 \leq R$ for all k under any of the following sets of assumptions:*

1. $r(x) = 0$, $f(x)$ is coercive, $\|\mathbf{e}_k\|_2 \leq \varepsilon_{\text{rel}} \|\mathbf{g}_k\|_2$, $\alpha < 2/L$, and $\varepsilon_{\text{rel}} \leq (2 - L\alpha)/(4 - L\alpha)$.
2. $r(x)$ is convex, $\sum_{k=0}^{\infty} \|\mathbf{e}_k\|_2 = E_{\infty} < \infty$, and $\alpha < 1/L$.
3. $F(x) = f(x) + r(x)$ is restricted-strongly convex, $\|\mathbf{e}_k\|_2 \leq \varepsilon_{\text{abs}}$, and $\alpha < 1/L$.
4. $F(x) = f(x) + r(x)$ is coercive with respect to $\|x\|_2$, $\partial F(x)$ is coercive with respect to $F(x)$ (see Definition 3), $\|\mathbf{e}_k\|_2 \leq \varepsilon_{\text{abs}}$, $F(x)$ satisfies Assumption 3 and $\alpha < 1/L$.

Proof. By the definition of x_{k+1} , we have for $y_k := x_k - \alpha \hat{\mathbf{g}}_k$:

$$r(x) + \frac{1}{2\alpha} \|x - y_k\|_2^2 \geq r(x_{k+1}) + \frac{1}{2\alpha} \|x_{k+1} - y_k\|_2^2$$

for all x . Rearranging it yields

$$r(x) - r(x_{k+1}) + \frac{1}{\alpha} \langle x_{k+1} - y_k, x - x_{k+1} \rangle + \frac{1}{2\alpha} \|x - x_{k+1}\|_2^2 \geq 0, \quad \forall x.$$

When r is convex, we directly have

$$r(x) - r(x_{k+1}) + \frac{1}{\alpha} \langle x_{k+1} - y_k, x - x_{k+1} \rangle \geq 0, \quad \forall x,$$

which follows from the inner-product between $\tilde{\nabla}r(x_{k+1}) + \frac{1}{\alpha}(x_{k+1} - y_k) = 0$ and $x - x_{k+1}$ and applying $r(x) - r(x_{k+1}) \geq \langle \tilde{\nabla}r(x_{k+1}), x - x_{k+1} \rangle$. By defining 1_{ncvx} to be equal to 1 if $r(x)$ is non-convex, and zero otherwise, we may summarize this as:

$$r(x) - r(x_{k+1}) + \frac{1}{\alpha} \langle x_{k+1} - y_k, x - x_{k+1} \rangle + \frac{1_{\text{ncvx}}}{2\alpha} \|x - x_{k+1}\|_2^2 \geq 0, \quad \forall x. \quad (30)$$

On the other hand:

$$\begin{aligned} f(x) - f(x_{k+1}) + \frac{L}{2} \|x_{k+1} - x_k\|_2^2 &= f(x) - f(x_k) + f(x_k) - f(x_{k+1}) + \frac{L}{2} \|x_{k+1} - x_k\|_2^2 \\ &\geq \langle \mathbf{g}_k, x - x_k \rangle + \langle \mathbf{g}_k, x_k - x_{k+1} \rangle = \langle \mathbf{g}_k, x - x_{k+1} \rangle, \end{aligned} \quad (31)$$

where we have used Assumptions 3 and the convexity of $f(x)$. Now adding equations (30) and (31), and using:

$$\frac{1}{\alpha} \langle x_{k+1} - y_k, x - x_{k+1} \rangle - \langle \mathbf{g}_k, x - x_{k+1} \rangle = \frac{1}{\alpha} \langle x_{k+1} - x_k, x - x_{k+1} \rangle + \langle \mathbf{e}_k, x - x_{k+1} \rangle$$

give us

$$\begin{aligned} F(x) - F(x_{k+1}) + \frac{1}{\alpha} \langle x_{k+1} - x_k, x - x_{k+1} \rangle \\ + \frac{L}{2} \|x_{k+1} - x_k\|_2^2 + \langle \mathbf{e}_k, x - x_{k+1} \rangle + \frac{1_{\text{ncvx}}}{2\alpha} \|x - x_{k+1}\|_2^2 \geq 0, \quad \forall x. \end{aligned} \quad (32)$$

In (32), choosing $x = x_k$, $x = P_*(x_0)$, $x = P_*(x_k)$ leads to different analyses. Note that $P_*(x_0)$ and $P_*(x_k)$ are both solutions but may be different.

Part 1: set $x = x_k$ and $r(x) = 0$ Under these assumptions, and recalling that $c_0 := \frac{1}{\alpha} - \frac{1}{L}$, (32) becomes:

$$\begin{aligned} f(x_k) - f(x_{k+1}) &\geq c_0 \|x_{k+1} - x_k\|_2^2 - \langle \mathbf{e}_k, x_k - x_{k+1} \rangle \\ &\geq c_0 \|x_{k+1} - x_k\|_2^2 - \left(\frac{c_0}{2} \|x_{k+1} - x_k\|_2^2 + \frac{1}{2c_0} \|\mathbf{e}_k\|_2^2 \right) \\ &= \frac{c_0}{2} \|x_{k+1} - x_k\|_2^2 - \frac{1}{2c_0} \|\mathbf{e}_k\|_2^2 \end{aligned}$$

where we have used Young's inequality. Under the assumption $\|\mathbf{e}_k\|_2 \leq \varepsilon_{\text{rel}} \|\mathbf{g}_k\|_2$ one can easily show that:

$$\|\mathbf{e}_k\|_2 \leq \frac{\varepsilon_{\text{rel}}}{1 - \varepsilon_{\text{rel}}} \|\hat{\mathbf{g}}_k\|_2 = \frac{\varepsilon_{\text{rel}}}{1 - \varepsilon_{\text{rel}}} \|x_{k+1} - x_k\|_2.$$

and hence:

$$\begin{aligned} f(x_k) - f(x_{k+1}) &\geq \frac{c_0}{2} \|x_{k+1} - x_k\|_2^2 - \frac{1}{2c_0} \frac{\varepsilon_{\text{rel}}^2}{(1 - \varepsilon_{\text{rel}})^2} \|x_{k+1} - x_k\|_2^2 \\ &= \left(\frac{c_0}{2} - \frac{\varepsilon_{\text{rel}}^2}{2\alpha^2 c_0 (1 - \varepsilon_{\text{rel}})^2} \right) \|x_k - x_{k+1}\|_2^2 \end{aligned}$$

Recalling that $c_0 = \frac{1}{\alpha} - \frac{L}{2}$ we see that for $\alpha < 2/L$ and $\varepsilon_{\text{rel}} \leq (2 - L\alpha)/(4 - L\alpha)$ the sequence $\{f(x_k)\}$ is monotonically decreasing. By coercivity, there exists an R such that $\|x_k - P_*(x_k)\|_2 \leq R$ for all k .

Part 2: set $x = P_*(x_0)$. This is a variation of (Schmidt et al., 2011, Sec. 6.1). Note however that there they assume $P_*(x_k) = x_*$ for all k . For completeness, we give some simplified steps. If $x = P_*(x_0)$ then (32) becomes:

$$\begin{aligned} \frac{1}{\alpha} \langle x_{k+1} - x_k, P_*(x_0) - x_{k+1} \rangle + \frac{L}{2} \|x_{k+1} - x_k\|_2^2 \\ + \langle \mathbf{e}_k, P_*(x_0) - x_{k+1} \rangle \geq F(x_{k+1}) - F(P_*(x_0)) \geq 0. \end{aligned} \quad (33)$$

Multiplying by 2α and substituting

$$2\langle x_{k+1} - x_k, P_*(x_0) - x_{k+1} \rangle = \|x_k - P_*(x_0)\|_2^2 - \|x_{k+1} - P_*(x_0)\|_2^2 - \|x_{k+1} - x_k\|_2^2 \quad (34)$$

yields:

$$\|x_k - P_*(x_0)\|_2^2 \geq \|x_{k+1} - P_*(x_0)\|_2^2 + (1 - \alpha L)\|x_{k+1} - x_k\|_2^2 - 2\alpha\langle \mathbf{e}_k, P_*(x_0) - x_{k+1} \rangle$$

Because $\alpha \leq 1/L$ we may drop the second term on the right hand side. Adding the inequality over $k = 0, \dots, K-1$ and apply telescopic cancellation we get:

$$\begin{aligned} \|x_0 - P_*(x_0)\|_2^2 &\geq \|x_K - P_*(x_0)\|_2^2 - 2\alpha \sum_{k=0}^{K-1} \langle \mathbf{e}_k, P_*(x_0) - x_{k+1} \rangle \\ &\geq \|x_K - P_*(x_0)\|_2^2 - 2\alpha \sum_{k=0}^{K-1} \|\mathbf{e}_k\|_2 \|P_*(x_0) - x_{k+1}\|_2. \end{aligned}$$

Since $E_k := \sum_{i=0}^{k-1} \|\mathbf{e}_i\|_2 \leq E_\infty$, by Lemma 1 of (Schmidt, Le Roux, Bach), we get

$$\begin{aligned} \|x_k - P_*(x_k)\|_2 &\leq \|x_k - P_*(x_0)\|_2 \leq \alpha E_k + ((\alpha E_k)^2 + \|x_0 - P_*(x_0)\|_2^2)^{1/2} \\ &\leq \alpha E_\infty + ((\alpha E_\infty)^2 + \|x_0 - P_*(x_0)\|_2^2)^{1/2}. \end{aligned}$$

Part 3: set $x = P_*(x_k)$ in (32). We get

$$\frac{1}{\alpha} \langle x_{k+1} - x_k, P_*(x_k) - x_{k+1} \rangle + \frac{L}{2} \|x_{k+1} - x_k\|_2^2 + \langle \mathbf{e}_k, P_*(x_k) - x_{k+1} \rangle \geq F(x_{k+1}) - F(P_*(x_k)). \quad (35)$$

Applying $F(P_*(x_k)) = F(P_*(x_{k+1}))$ and then using restricted strong convexity (Assumption 2) $F(x_{k+1}) - F(P_*(x_{k+1})) \geq \nu \|x_{k+1} - P_*(x_{k+1})\|^2$, one can strengthen (35) to

$$\frac{1}{\alpha} \langle x_{k+1} - x_k, P_*(x_k) - x_{k+1} \rangle + \frac{L}{2} \|x_{k+1} - x_k\|_2^2 \geq \nu \|x_{k+1} - P_*(x_{k+1})\|_2^2 - \langle \mathbf{e}_k, P_*(x_k) - x_{k+1} \rangle.$$

Multiplying both sides by 2α and substituting the following identity

$$2\langle x_{k+1} - x_k, P_*(x_k) - x_{k+1} \rangle = \|x_k - P_*(x_k)\|_2^2 - \|x_{k+1} - P_*(x_k)\|_2^2 - \|x_{k+1} - x_k\|_2^2$$

gives us:

$$\begin{aligned} \|x_k - P_*(x_k)\|_2^2 &\geq 2\alpha\nu \|x_{k+1} - P_*(x_{k+1})\|_2^2 + \|x_{k+1} - P_*(x_k)\|_2^2 \\ &\quad + (1 - \alpha L)\|x_{k+1} - x_k\|_2^2 - 2\alpha\langle \mathbf{e}_k, P_*(x_k) - x_{k+1} \rangle \end{aligned}$$

Because $\alpha \leq 1/L$ we may drop the term proportional to $\|x_{k+1} - x_k\|_2^2$ since $1 - \alpha L \geq 0$. Applying Young's inequality to the last term:

$$\begin{aligned} \|x_k - P_*(x_k)\|_2^2 &\geq 2\alpha\nu \|x_{k+1} - P_*(x_{k+1})\|_2^2 + \|x_{k+1} - P_*(x_k)\|_2^2 - \alpha\nu \|x_{k+1} - P_*(x_k)\|_2^2 - \frac{\alpha}{\nu} \|\mathbf{e}_k\|_2^2 \\ &= 2\alpha\nu \|x_{k+1} - P_*(x_{k+1})\|_2^2 + (1 - \alpha\nu) \|x_{k+1} - P_*(x_k)\|_2^2 - \frac{\alpha}{\nu} \|\mathbf{e}_k\|_2^2. \end{aligned}$$

By $\nu \leq L$ and $\alpha \leq 1/L$, we get $1 - \alpha\nu \geq 0$. Apply this with $\|x_{k+1} - P_*(x_k)\|_2 \geq \|x_{k+1} - P_*(x_{k+1})\|_2$:

$$\|x_k - P_*(x_k)\|_2^2 \geq (1 - \alpha\nu)\|x_{k+1} - P_*(x_{k+1})\|_2^2 - \frac{\alpha}{\nu}\|\mathbf{e}_k\|_2^2.$$

This inequality matches the form $(b - a)e_k \geq be_{k+1} - c_k$ of Proposition B.2, which yields the bound

$$\|x_k - P_*(x_k)\|_2^2 \leq \frac{1}{(1 - \alpha\nu)^k} \|x_0 - P_*(x_0)\|_2^2 + \sum_{t=1}^k \frac{\alpha}{(1 - \alpha\nu)^t \nu} \|\mathbf{e}_k\|_2^2.$$

With $\|\mathbf{e}_k\| \leq \varepsilon_{\text{abs}}$, we get

$$\|x_k - P_*(x_k)\|_2^2 \leq \frac{1}{(1 + \alpha\nu)^k} \|x_0 - P_*(x_0)\|_2^2 + \frac{\varepsilon_{\text{abs}}}{\nu^2}.$$

Part 4. From (23) we have that:

$$F(x_{k+1}) - F(x_k) \leq -c_3\alpha^2 \|\tilde{\Delta}_k\|_2^2 + c_4\|\mathbf{e}_k\|_2^2 \leq -c_3\alpha^2 \|\tilde{\Delta}_k\|_2^2 + c_4\varepsilon_{\text{abs}}^2 \quad (36)$$

where we are also using the assumption $\|\mathbf{e}_k\|_2 \leq \varepsilon_{\text{abs}}$. By definition, $-\tilde{\Delta}_k \in \partial F(x_{k+1})$ and hence by coercivity of ∂F with respect to F , there exists an R_1 such that $F(x_{k+1}) > R_1$ implies that $\|\tilde{\Delta}_k\|_2^2 > \frac{c_4\varepsilon_{\text{abs}}^2}{c_3\alpha^2}$. This in turn implies that the right-hand side of (36) is strictly negative. Therefore, by induction, $F(x_k) \leq \max\{F(x_0), R_1\}$ for all $k \geq 0$. Finally, by coercivity of $F(x)$ with respect to $\|x\|_2$ and the fact that $\{F(x_k)\}_{k=0}^\infty$ is bounded, $\{\|x_k\|_2\}_{k=1}^\infty$ is bounded. It then follows that $\{\|x_k - P_*(x_k)\|_2\}_{k=1}^\infty$ is bounded. \square

C Proofs for Section 5

Proof of Theorem 5.1. Applying Theorem 3.2 with $\sigma = 0$ yields

$$\begin{aligned} \|\mathbf{g}_k - \hat{\mathbf{g}}_k\|_2 &\leq \frac{\tau\delta_k H}{2} + (\psi + \rho^n)\|\mathbf{g}_k\|_2 \\ &= \left(\frac{\tau\delta_k H}{2(\varepsilon_{\text{rel}} - \psi - \rho^n)\|\mathbf{g}_k\|_2} \right) (\varepsilon_{\text{rel}} - \psi - \rho^n)\|\mathbf{g}_k\|_2 + (\psi + \rho^n)\|\mathbf{g}_k\|_2, \end{aligned}$$

for all k with probability $1 - (s/d)^{b_2 s}$. Now, to guarantee that $\|\mathbf{g}_k - \hat{\mathbf{g}}_k\|_2 \leq \varepsilon_{\text{rel}}\|\mathbf{g}_k\|_2$ we need to choose

$$\delta_k \leq \frac{2(\varepsilon_{\text{rel}} - \psi - \rho^n)\|\mathbf{g}_k\|_2}{\tau H}. \quad (37)$$

Of course, we do not have access to $\|\mathbf{g}_k\|_2$ when choosing δ_k ; hence, we use $\|\hat{\mathbf{g}}_{k-1}\|_2$ as a proxy. We use the inductive assumption that $\|\mathbf{g}_{k-1} - \hat{\mathbf{g}}_{k-1}\|_2 \leq \varepsilon_{\text{rel}}\|\mathbf{g}_{k-1}\|_2$, in which case we have that:

$$\begin{aligned} \|\hat{\mathbf{g}}_{k-1}\|_2 &= \|\hat{\mathbf{g}}_{k-1} - \mathbf{g}_{k-1} + \mathbf{g}_{k-1} - \mathbf{g}_k + \mathbf{g}_k\|_2 \\ &\leq \|\hat{\mathbf{g}}_{k-1} - \mathbf{g}_{k-1}\|_2 + \|\mathbf{g}_{k-1} - \mathbf{g}_k\|_2 + \|\mathbf{g}_k\|_2 \\ &\leq \varepsilon_{\text{rel}}\|\mathbf{g}_{k-1}\|_2 + L\|x_k - x_{k-1}\|_2 + \|\mathbf{g}_k\|_2 \end{aligned} \quad (38)$$

Because $x_k = x_{k-1} - \alpha\hat{\mathbf{g}}_{k-1}$ we have that $L\|x_k - x_{k-1}\|_2 \leq \alpha L\|\hat{\mathbf{g}}_{k-1}\|_2$. Moreover, one can easily show that:

$$\|\mathbf{g}_{k-1}\|_2 \leq \frac{1}{1 - \varepsilon_{\text{rel}}} \|\hat{\mathbf{g}}_{k-1}\|_2$$

Thus equation (38) becomes

$$\begin{aligned}\|\hat{\mathbf{g}}_{k-1}\|_2 &\leq \frac{\varepsilon_{\text{rel}}}{1 - \varepsilon_{\text{rel}}} \|\hat{\mathbf{g}}_{k-1}\|_2 + \alpha L \|\hat{\mathbf{g}}_{k-1}\|_2 + \|\mathbf{g}_k\|_2 \\ &\Rightarrow \left(\frac{1 - \alpha L - \varepsilon_{\text{rel}}(2 - \alpha L)}{1 - \varepsilon_{\text{rel}}} \right) \|\hat{\mathbf{g}}_{k-1}\|_2 \leq \|\mathbf{g}_k\|_2\end{aligned}$$

and so to guarantee (37), it suffices to choose

$$\begin{aligned}\delta_k &\leq \frac{2(\varepsilon_{\text{rel}} - \psi - \rho^n)(1 - L\alpha - \varepsilon_{\text{rel}}(2 - \alpha L))}{\tau H(1 - \varepsilon_{\text{rel}})} \|\hat{\mathbf{g}}_{k-1}\|_2 \\ &=: \beta \|\hat{\mathbf{g}}_{k-1}\|_2.\end{aligned}$$

Note that this condition is only meaningful when $\beta > 0$, thus we require that:

$$\psi + \rho^n < \varepsilon_{\text{rel}} < \frac{1 - \alpha L}{2 - \alpha L} \quad \text{and } \alpha < \frac{1}{L}.$$

□

Theorem 5.1 requires that $\|\mathbf{g}_0 - \hat{\mathbf{g}}_0\|_2 \leq \varepsilon_{\text{rel}} \|\mathbf{g}_0\|_2$. Let us briefly discuss how one can guarantee this. From Theorem A.4 we get that with probability $1 - e^{-m/24}$:

$$\begin{aligned}\|Z(\mathbf{g}_0 - \hat{\mathbf{g}}_0)\|_2^2 &\geq \frac{1}{2} \|\mathbf{g}_0 - \hat{\mathbf{g}}_0\|_2^2 \\ \Rightarrow \|\mathbf{g}_0 - \hat{\mathbf{g}}_0\|_2 &\leq \sqrt{2} \|Z\mathbf{g}_0 - Z\hat{\mathbf{g}}_0\|_2 \\ &\stackrel{(a)}{=} \sqrt{2} \|(\mathbf{y} + \delta\nu) - Z\hat{\mathbf{g}}_0\|_2 \\ &\stackrel{(b)}{\leq} \sqrt{2} \left(\|\mathbf{y} - Z\hat{\mathbf{g}}_0\|_2 + \frac{H\delta}{2} \right)\end{aligned}$$

where (a) follows from (18) with $\sigma = 0$ and (b) follows from Lemma A.6. On the other hand:

$$\begin{aligned}\|\mathbf{y}\|_2 &\stackrel{(a)}{=} \|Z\mathbf{g}_0 + \delta\nu\|_2 \\ &\stackrel{(b)}{\leq} \|Z\mathbf{g}_0\|_2 + \frac{H\delta}{2} \\ &\stackrel{(c)}{\leq} \sqrt{2} \|\mathbf{g}_0\|_2 + \frac{H\delta}{2},\end{aligned}$$

where again (a) follows from (18) and (b) from Lemma A.6 while (c) holds with probability $1 - e^{-m/12}$ by Theorem A.4. It follows that:

$$\frac{1}{\sqrt{2}} \left(\|\mathbf{y}\|_2 - \frac{H\delta}{2} \right) \leq \|\mathbf{g}_0\|_2$$

and thus if:

$$\begin{aligned}\sqrt{2} \left(\|\mathbf{y} - Z\hat{\mathbf{g}}_0\|_2 + \frac{H\delta}{2} \right) &\leq \frac{\varepsilon_{\text{rel}}}{\sqrt{2}} \left(\|\mathbf{y}\|_2 - \frac{H\delta}{2} \right) \\ \iff \|\mathbf{y} - Z\hat{\mathbf{g}}_0\|_2 &\leq \frac{\varepsilon_{\text{rel}}}{2} \|\mathbf{y}\|_2 - \left(1 + \frac{\varepsilon_{\text{rel}}}{2} \right) \left(\frac{H\delta}{2} \right),\end{aligned}$$

then with probability $1 - e^{-m/12} - e^{-m/24}$ we indeed have that $\|\mathbf{g}_0 - \hat{\mathbf{g}}_0\|_2 \leq \varepsilon_{\text{rel}}\|\mathbf{g}_0\|_2$. This condition is checkable, assuming we have a good estimate of H . Furthermore, it must hold for δ sufficiently small. Thus, we recommend starting with some initial estimate δ_0 and performing a decreasing binary search over $(0, \delta_0)$ until a δ is found such that this condition holds.

Proof of Corollary 5.2. **Part 1:** By assumption, we may choose ε_{rel} and n satisfying:

$$\psi + \rho^n < \varepsilon_{\text{rel}} < \frac{1 - \alpha L}{2 - \alpha L}$$

hence by Theorem 5.1, $\|\mathbf{g}_k - \hat{\mathbf{g}}_k\|_2 \leq \varepsilon_{\text{rel}}\|\mathbf{g}_k\|_2$ for all k . Since in addition $\varepsilon_{\text{rel}} \leq (2 - \alpha L)/(4 - \alpha L)$, from Proposition B.6, $\|\mathbf{x}_k - \mathbf{P}_*(\mathbf{x}_k)\|_2 \leq R$ for some fixed R . The stated convergence rate then follows from Theorem 4.1.

Part 2: follows from combining Theorems 5.1 and 4.2. \square

Proof of Theorem 5.3. Appealing again to Theorem 3.2, this time with $\sigma = 0$ and $\psi = 0$, we get

$$\|\mathbf{g}_k - \hat{\mathbf{g}}_k\|_2 \leq \frac{\tau \delta_k H}{2} + \rho^n \|\mathbf{g}_k\|_2$$

for all k . Because \mathbf{g}_k is s -sparse:

$$\begin{aligned} \|\mathbf{g}_k\|_2 &\stackrel{(a)}{\leq} \frac{1}{\sqrt{1 - \delta_s(Z)}} \|Z\mathbf{g}_k\|_2 \\ &\stackrel{(b)}{\leq} \frac{1}{\sqrt{1 - \delta_s(Z)}} (\|\mathbf{y}_k\|_2 + \delta_k \|\boldsymbol{\nu}\|_2) \\ &\stackrel{(c)}{\leq} \frac{1}{\sqrt{1 - \delta_s(Z)}} \left(\|\mathbf{y}_k\|_2 + \frac{\delta_k H}{2} \right) \\ &\stackrel{(d)}{\leq} \sqrt{2} \left(\|\mathbf{y}_k\|_2 + \frac{\delta_k H}{2} \right) \end{aligned}$$

where (a) follows from the definition of the RIP (see discussion below Theorem A.1), (b) follows from (18), (c) follows from Lemma A.6 and (d) is because $\delta_s(Z) \leq \delta_{4s}(Z) \leq 0.5$ by Theorem A.1. Choosing n sufficiently large (specifically $n = \frac{\log(\delta_k H/2) - \log(\sqrt{2}(\|\mathbf{y}\|_k + \delta_k H/2))}{\log(\rho)}$) we obtain:

$$\|\mathbf{g}_k - \hat{\mathbf{g}}_k\|_2 \leq \frac{\tau \delta_k H}{2} + \frac{\tau \delta_k H}{2} \leq \frac{\tau H}{k^{1.1}}$$

given the choice of δ_k . \square

Proof of Corollary 5.4. By Theorem 5.3:

$$\sum_{k=1}^{\infty} \|\mathbf{g}_k - \hat{\mathbf{g}}_k\|_2 \leq \tau H \sum_{k=1}^{\infty} k^{-1.1} = E_{\infty}^1 < \infty$$

Now apply Proposition 1 of (Schmidt et al., 2011) with $x_* = P_*(x_0)$. \square

Proof of Corollary 5.6. This follows from Theorem 4.3 Part 1 because by Theorem 5.3:

$$E_K^2 := \sum_{k=1}^K \|\mathbf{g}_k - \hat{\mathbf{g}}_k\|_2^2 = C\tau H \sum_{k=1}^{\infty} k^{-1.1} := E_{\infty}^K < \infty.$$

□

Proof of Theorem 5.7. From Theorem 3.2 we obtain:

$$\|\mathbf{g}_k - \hat{\mathbf{g}}_k\|_2 \leq \frac{2\tau\sigma}{\delta} + \frac{\tau\delta H}{2} + \rho^n \|\mathbf{g}_k\|_2$$

with probability $1 - (s/d)^{b_2 s}$. Using the same trick as in the proof of Theorem 5.3 we can guarantee that $\rho^n \|\mathbf{g}_k\|_2 \leq \tau\delta H/2$ for n sufficiently large and so:

$$\|\mathbf{g}_k - \hat{\mathbf{g}}_k\|_2 \leq \frac{2\tau\sigma}{\delta} + \tau\delta H$$

Optimizing the right hand side in terms of δ we obtain that $\|\mathbf{g} - \hat{\mathbf{g}}\|_2 \leq 2\sqrt{2\tau\sigma H}$ and that this is achieved when $\delta = \sqrt{2\sigma/H}$ □

Proof of Corollary 5.8. From Theorem 5.7, we get that $\|\mathbf{g}_k - \hat{\mathbf{g}}_k\|_2 \leq 2^{3/2} \sqrt{\tau\sigma H}$ for all $k = 1, \dots, K$ with probability $1 - (s/d)^{b_2 s}$. The first claim follows by combining this with Theorem 4.1 part 1. Note that $\|\mathbf{x}_k - \mathbf{P}_*(\mathbf{x}_k)\|_2 \leq R$ for all k by Proposition B.6 part 4. The second claim follows from combining the estimate $\|\mathbf{g}_k - \hat{\mathbf{g}}_k\|_2 \leq 2^{3/2} \sqrt{\tau\sigma H}$ with Theorem 4.2 part 1. □

Proof of Corollary 5.9. This follows from Theorem 4.3 Part 2 with $\varepsilon_{\text{abs}} = 2\sqrt{2\tau\sigma H}$, which is guaranteed by Theorem 5.7. □

Proof of Theorem 5.10. By the assumptions on $\|\mathbf{g}_0 - \hat{\mathbf{g}}_0\|_2$ and the fact that $\varepsilon_{\text{rel}} < \min_{i:(g_0)_i \neq 0} |(g_0)_i| / \|\mathbf{g}_0\|_2$ we have that:

$$\min_{i:(g_0)_i \neq 0} |(g_0)_i| > \|\mathbf{g}_0 - \hat{\mathbf{g}}_0\|_2 \Rightarrow \hat{S}_0 := \text{supp}(\hat{\mathbf{g}}_0) = \text{supp}(\mathbf{g}_0) =: S.$$

Now assume that $\hat{S}_{k-1} = S$. We claim that Algorithm 4 will return $\hat{\mathbf{g}}_k$ satisfying $\hat{S}_k := \text{supp}(\hat{\mathbf{g}}_k) = S$ and $\|\mathbf{g}_k - \hat{\mathbf{g}}_k\|_2 \leq \varepsilon_{\text{rel}} \|\mathbf{g}_k\|_2$ while making only s oracle queries. To see this, let Z_S denote the submatrix of Z containing only the columns indexed by S . Observe that Z_S is invertible, almost surely, and that $\lambda_{\min}(Z_S) \geq \varepsilon_{\text{inv}} / \sqrt{s}$ with probability at least $1 - O(\varepsilon_{\text{inv}})$ (see Theorem A of (Tikhomirov, 2020)). Let $\hat{\mathbf{g}}$ be the solution to the support-constrained least squares problem in line 5 of Algorithm 4. Then:

$$[\hat{\mathbf{g}}]_S = Z_S^{-1} \mathbf{y} = Z_S^{-1} (Z \mathbf{g}_k + \delta \sqrt{s} \boldsymbol{\nu}).$$

Using (18). Note the discrepancy here: in (18) $\boldsymbol{\nu} \in \mathbb{R}^m$ whereas here $\boldsymbol{\nu} \in \mathbb{R}^s$ and has entries $\nu_i = z_i^\top \nabla^2 f(x + tz_i) z_i / \sqrt{s}$ for some $t \in (0, 1)$. Continuing:

$$\begin{aligned} [\hat{\mathbf{g}}]_S &= Z_S^{-1} (Z_S [\mathbf{g}_k]_S + \delta \sqrt{s} \boldsymbol{\nu}) \quad (\text{As } \text{supp}(\mathbf{g}_k) = S) \\ &= [\mathbf{g}_k]_S + \delta \sqrt{s} Z_S^{-1} \boldsymbol{\nu}. \end{aligned}$$

Hence, $\|Z\hat{\mathbf{g}} - \mathbf{y}\|_2 = 0$ and $\hat{\mathbf{g}}$ is always accepted as the output of Algorithm 4 in lines 6–8 (i.e. $\hat{g}_k = \hat{g}$). Thus indeed Algorithm 4 makes s oracle queries, and by construction $\text{supp}(\hat{\mathbf{g}}_k) = S$. Moreover:

$$\|\hat{\mathbf{g}} - \mathbf{g}_k\|_2 \leq \delta\sqrt{s}\|Z_S^{-1}\boldsymbol{\nu}\|_2 \leq \delta\sqrt{s}\|Z_S^{-1}\|_2\|\boldsymbol{\nu}\|_2 \leq \delta\sqrt{s}(\lambda_{\min}(Z_S))^{-1}\frac{H}{2} \leq \delta\frac{sH}{2\varepsilon_{\text{inv}}},$$

where the last inequality holds with probability at least $1 - O(\varepsilon_{\text{inv}})$. As in the proof of Theorem 3.2 we obtain:

$$\left(\frac{1 - \alpha L - \varepsilon_{\text{rel}}(2 - \alpha L)}{1 - \varepsilon_{\text{rel}}}\right)\|\hat{\mathbf{g}}_{k-1}\|_2 \leq \|\mathbf{g}_k\|_2$$

and hence with the choice of β stated we get that:

$$\|\hat{\mathbf{g}} - \mathbf{g}_k\|_2 \leq \varepsilon_{\text{rel}}\|\mathbf{g}_k\|_2 \quad \text{for all } k, \text{ with probability at least } 1 - O(\varepsilon_{\text{inv}}). \quad (39)$$

Note that because $\varepsilon < (1 - L\alpha)/(2 - L\alpha)$ we have that $\beta > 0$. Because $\varepsilon_{\text{rel}} \leq (2 - L\alpha)/(4 - L\alpha)$ it again follows from Proposition B.6, $\|x_k - \mathbf{P}_*(x_k)\|_2 \leq R$ for some fixed R . Now appealing to Part 2 of Theorem 4.1 with $K = T/s$, we get that:

$$e_K \leq \frac{c_9 e_0 R^2}{T e_0 / b_1 s + c_9 R^2} = O\left(\frac{s}{T}\right)$$

where b_1 is defined as in Lemma A.1. □

D More Numerical Results

D.1 Synthetic example

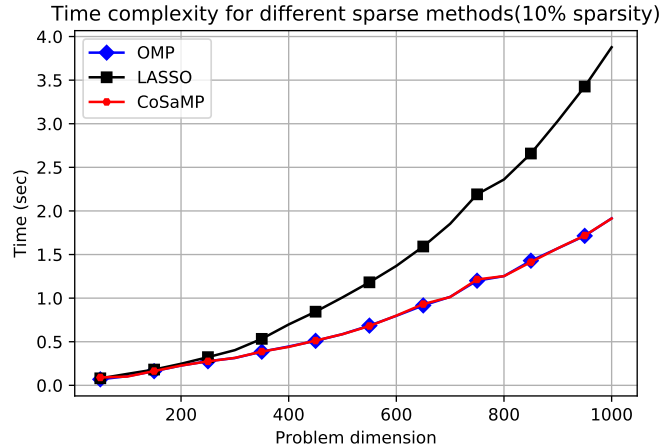


Figure 5: Running time *v.s.* problem dimension for different sparse methods when the sparsity ratio is fixed.

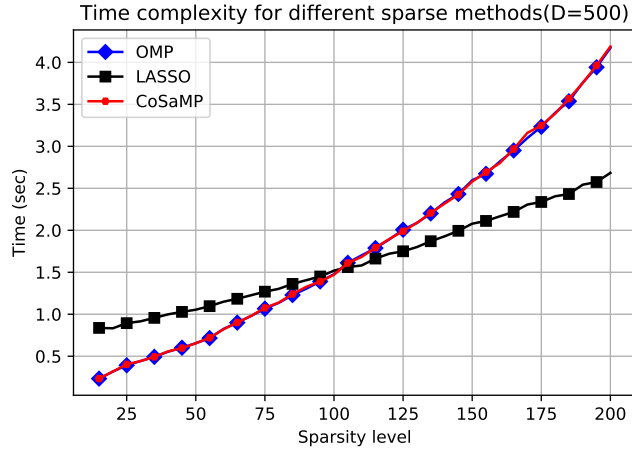


Figure 6: Running time *v.s.* sparsity level for different sparse methods when the problem dimension is fixed.

We investigate the runtime of ZORO with different sparse gradient estimators (*i.e.*, estimating the sparse gradients with OMP, LASSO or CoSaMP). The experiments are executed in MATLAB R2019a on a Windows 10 laptop with Intel i7-8750H CPU (6 cores at 2.2GHz) and 32GB of RAM. We implement all three versions of ZORO by ourselves. In particular, for the LASSO based gradient estimator, we use FISTA to be solver, and choose the regularizing parameter λ_{k+1} at $(k+1)$ -th iteration by the ratio of the ℓ_2 residual squared and ℓ_1 -norm from the last iteration: $\lambda_{k+1} = c\|\mathbf{y}_k - Z_k \hat{\mathbf{g}}_k\|_2^2 / \|\hat{\mathbf{g}}_k\|_1$, where c is a fixed parameter throughout all iterations. Furthermore, the stop criteria of all three gradient estimators are set to $\|\mathbf{x}_{k+1} - \mathbf{x}_k\|_2 / \|\mathbf{x}_k\|_2 \leq 10^{-6}$.

We consider the problem of minimizing a quadratic function $f(\mathbf{x}) = \mathbf{x}^\top \mathbf{A} \mathbf{x} / 2$, where $\mathbf{A} \in \mathbb{R}^{d \times d}$ is a diagonal matrix with s non-zero randomly generated positive elements. The runtime is evaluated with varying problem dimension (see Figure 5) and sparsity level (see Figure 6). Moreover, the runtimes reported in Figures 5 and 6 are based on 30 iterations of gradient descent, and averaged over 10 random tests. We find that the greedy methods, CoSaMP and OMP, have a speed advantage when the problem dimension is large and sparsity level is small, while the LASSO solver is fastest when both d and s are small. We emphasize that the gradients estimated by all three methods offer almost identical convergence performance on these easier synthetic tasks, so the stopping criterion of ZORO will not affect our observations.

D.2 Sparse adversarial attack on ImageNet

For this numerical experiment, we use the code from <https://github.com/KaidiXu/Z0-AdaMM> with a few modifications. We focus on the per-image untargeted attack scenario. For the objective function, we change the ℓ_2 -norm of distortion to ℓ_0 -norm. At each iteration, we randomly select a subspace of 2000 variables and generate 50 random Rademacher perturbation signals in this subspace. We use a much larger step-size than (Chen et al., 2019) since our gradient estimate has much better precision. Note that there are several hyper-parameters (step-size, decay parameter, subspace dimension, ZORO parameters, etc.) that have not been fully optimized. We plan to

address this issue along with more diverse simulation settings (targeted attacks, universal attacks, etc.) in a future work. We present some examples of successful sparse attack by ZORO in Figure 7.

Notice that the distortions are similar with impulse noise, which can be mitigated by a median filter. We use the tool `ndimage.median_filter` from `scipy`. We use \mathcal{A} to denote the set of adversarial images (original image+distortion) that are successfully attacked by ZORO. We use \mathcal{I}_1 to denote the set of image IDs that are not recovered. The ratio of images in \mathcal{A} been identified to the true label after filtering is the recover successful rate: $1 - |\mathcal{I}_1|/|\mathcal{A}|$. We then analyze the side-effect of median filter by apply it to the original images of \mathcal{A} . We use \mathcal{I}_2 to denote the set of image IDs that are mis-classified. The distortion rate is the ratio of images been assigned an incorrect label: $|\mathcal{I}_2|/|\mathcal{A}|$. We summarize the images indexes from these two experiments and calculate the total accuracy reduction: $|\mathcal{I}_1 \cup \mathcal{I}_2|/|\mathcal{A}|$. Note that there are some overlapping IDs in \mathcal{I}_1 and \mathcal{I}_2 .



(a) True label: "corn" → Mislabeled: "ear, spike, capitulum"



(b) True label: "plastic bag" → Mislabeled: "shower cap"



(c) True label: "water ouzel, dipper" → Mislabeled: "otter"



(d) True label: "thimble" → Mislabeled: "measuring cup"

Figure 7: Examples of adversarial images and the mis-classified labels.